Journal of Medicinal Chemistry

Article

pubs.acs.org/jmc

Structure–Affinity Relationships and Structure–Kinetic Relationships of 1,2-Diarylimidazol-4-carboxamide Derivatives as Human Cannabinoid 1 Receptor Antagonists

Lizi Xia,[†] Henk de Vries,[†] Eelke B. Lenselink,[†] Julien Louvel,[○,†] Michael J. Waring,[∥] Leifeng Cheng,[⊥] Sara Pahlén,[§] Maria J. Petersson,[§] Peter Schell,[#] Roine I. Olsson,[∇] Laura H. Heitman,[†] Robert J. Sheppard,[*,‡] and Adriaan P. IJzerman[*,†]

[†]Division of Medicinal Chemistry, LACDR, Leiden University, 2300RA Leiden, The Netherlands

[‡]Medicinal Chemistry, Oncology, IMED Biotech Unit, AstraZeneca, Cambridge SK10 2NA, United Kingdom

[§]Medicinal Chemistry, Cardiovascular and Metabolic Diseases, IMED Biotech Unit, AstraZeneca, Gothenburg SE-431 83, Sweden

S *Supporting Information*

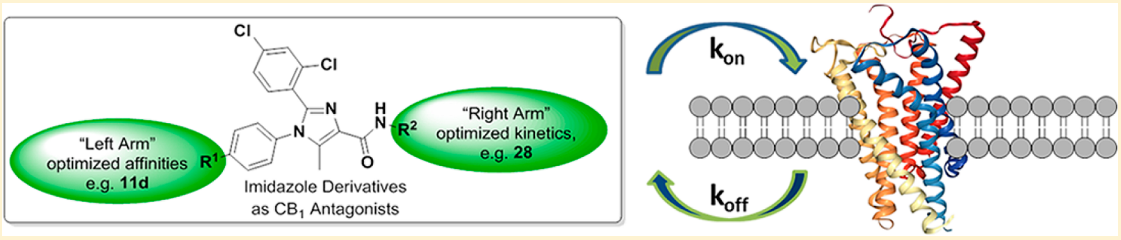

ABSTRACT: We report on the synthesis and biological evaluation of a series of 1,2-diarylimidazol-4-carboxamide derivatives developed as CB_1 receptor antagonists. These were evaluated in a radioligand displacement binding assay, a [^{35}S]GTPγS binding assay, and in a competition association assay that enables the relatively fast kinetic screening of multiple compounds. The compounds show high affinities and a diverse range of kinetic profiles at the CB_1 receptor and their structure–kinetic relationships (SKRs) were established. Using the recently resolved hCB_1 receptor crystal structures, we also performed a modeling study that sheds light on the crucial interactions for both the affinity and dissociation kinetics of this family of ligands. We provide evidence that, next to affinity, additional knowledge of binding kinetics is useful for selecting new hCB_1 receptor antagonists in the early phases of drug discovery.

INTRODUCTION

Within the endocannabinoid system (ECS), two human cannabinoid receptor subtypes have been identified: the human CB_1 (hCB_1) receptor and the human CB_2 (hCB_2) receptor.[1] They are members of the rhodopsin-like class A G-protein-coupled receptors (GPCRs) and are primarily activated by endogenous cannabinoids (endocannabinoids, ECs), including anandamide (or *N*-arachidonylethanolamine, AEA) and 2-arachidonoylglycerol (2-AG).[1,2] The hCB_1 and hCB_2 receptors show 44% overall sequence homology and display different pharmacological profiles.[3] The hCB_1 receptor is present in the central nervous system (CNS) and is widely distributed in the peripheral nervous system (PNS) and peripheral tissues,[2,4] including heart, liver, lung, gastrointestinal tract, pancreas, and adipose tissue.[5,6] The presence of the hCB_1 receptor within both the CNS and PNS mediates neurotransmitter release and controls various cognitive, motor, emotional, and sensory functions. Furthermore, activation in the peripheral tissues contributes to energy balance and metabolic processes.[6−9]

The broad presence of the hCB_1 receptor in a variety of complex physiological systems provides numerous opportunities for therapeutic intervention. In the particular case of obesity, the ECS, including the hCB_1 receptor, is overactive, with increased levels of endocannabinoids in plasma, both in central and peripheral tissues.[10] Therefore, blockade of the hCB_1 has been explored for the treatment of obesity. With this in mind, rimonabant (SR141716A, Figure 1a), a hCB_1 receptor inverse agonist, was developed by Sanofi-Aventis and introduced in Europe in 2006. However, it was quickly withdrawn from the market due to unacceptable psychiatric side effects.[11−13] Many other hCB_1 receptor antagonists entered into clinical trials, such as taranabant (MK-0364, Figure 1b)[14] and otenabant (CP945598, Figure 1c).[15] However, they were not developed further due to similar psychiatric side effects despite their diverse chemical structures.

To avoid the CNS side effects, peripherally acting hCB_1 receptor antagonists with physicochemical features that reduce brain penetration have been developed.[16] Another approach has been the development of hCB_1 receptor neutral antagonists because it has been postulated that the CNS side effects of rimonabant were due to its inverse agonism.[17−19]

Drug target binding kinetic parameters are receiving increasing attention, alongside classical affinity (K_i) and potency (IC_{50})

Received: June 13, 2017
Published: November 7, 2017

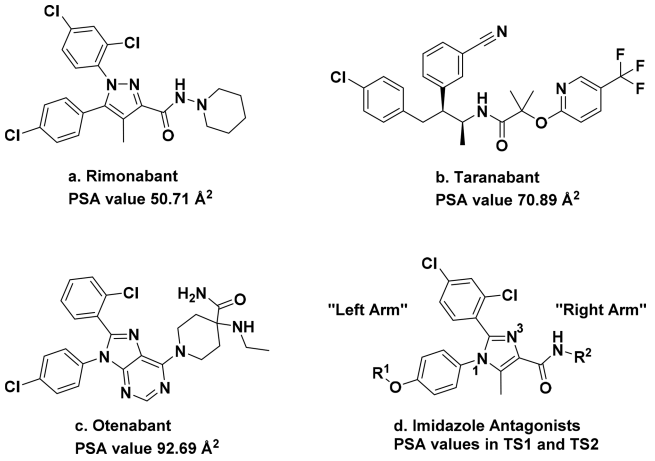

Figure 1. Chemical structures of (a) rimonabant, (b) taranabant, (c) otenabant, and (d) the scaffold of 1,2-diarylimidazol-4-carboxamides as CB_1 receptor antagonists; the R^1 substitution is defined as the "left arm" of the scaffold while the R^2 substitution defines the "right arm" of the scaffold. The calculations of PSA values are reported in Supporting Information.

values, as has been discussed for several other class A GPCRs. In particular, the receptor−ligand residence time (RT) is emerging as an additional parameter to assess the therapeutic potential of drug candidates with respect to drug efficacy and safety.[20−22] In the research field of GPCRs, a number of structure−kinetic relationship (SKR) studies have been published and the results suggest that the strategic combination of SKR with classic structure−affinity relationships (SAR) can improve the resulting decision process.[23−26] By doing so, ligand−receptor interactions can be better understood, as together they not only comprise the equilibrium state of a ligand−receptor interaction but also its metastable intermediates and/or transition states.[27] The binding kinetics driven drug discovery approach for the hCB_1 receptor has been validated in some aspects already by its application in the development of allosteric modulators of the hCB_1 receptor.[28,29]

In the current study, we report the synthesis and evaluation of 1,2-diarylimidazol-4-carboxamide derivatives (Figure 1d), as human CB_1 receptor antagonists with more polar characteristics than rimonabant.[30,31] Together with rimonabant, they were evaluated in a radioligand displacement assay, a [^{35}S]GTPγS binding assay, and a dual-point competition association assay that enables the relatively fast kinetic screening of compounds.[32] Selected compounds were progressed to a full competition association assay. The compounds show high affinities and a diverse range of kinetic profiles at the hCB_1 receptor, which allowed their structure−kinetic relationships (SKRs) to be established. Their putative binding mode was analyzed using the recently resolved crystal structures of the hCB_1 receptor,[33,34] shedding light on key structural features of the receptor binding site that are involved in ligand recognition and dissociation. Thus, we provide evidence that, in additional to affinity, knowledge of binding kinetics is useful for selecting new hCB_1 receptor antagonists in the early phases of drug discovery.

RESULTS AND DISCUSSION

Chemistry. The synthesis of the 1,2-diarylimidazol-4-carboxamide scaffold commenced from commercially available 4-(benzyloxy)aniline **1**, which was converted to the 2,4-dichlorobenzamidine **2** (Scheme 1). After a one-pot condensation and

Scheme 1. Synthesis of Antagonists 8a, 8b, and 11a−h[a]

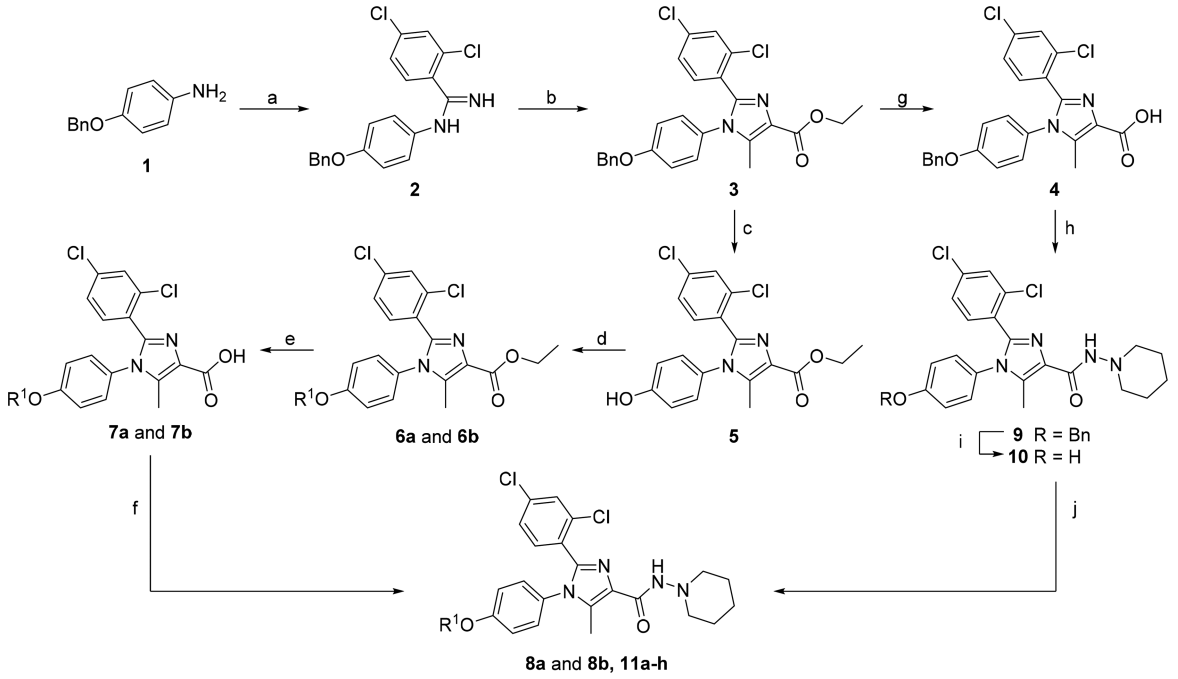

[a]Reagents and conditions: (a) EtMgBr, 2,4-diClPhCN, THF, rt, 20 h, 98%; (b) (i) $EtO_2CC(O)CH(Br)CH_3$, K_2CO_3, THF, rt, 66 h, (ii) AcOH, reflux, 1 h, 65%; (c) HBr, AcOH, rt, 15 h, 63%; (d) R^1-OH, DEAD, Ph_3P, THF, toluene, rt, 15 h, 77%; (e) KOH, EtOH:THF:H_2O 2:2:1, 50 °C, 3.5 h, 95%; (f) (i) $(COCl)_2$, DMF cat., CH_2Cl_2, rt, 90 min, (ii) piperidin-1-amine·HCl, pyridine, CH_2Cl_2, rt, 2 h, 55% (2 steps); (g) KOH, MeOH:H_2O 3:1, reflux, 2 h, 99%; (h) (i) $(COCl)_2$, DMF cat., CH_2Cl_2, reflux, 2 h, (ii) piperidin-1-amine, NEt_3, CH_2Cl_2, 0 °C to rt, 2 h, 74%; (i) BBr_3, CH_2Cl_2, rt, 1 h, 58%; (j) R^1-X, base, CH_2Cl_2. Corresponding 56−90% R^1 substitutions are listed in Table 1.

DOI: 10.1021/acs.jmedchem.7b00861
J. Med. Chem. 2017, 60, 9545−9564

Table 1. In Vitro Pharmacology Data, Including Conventional Antagonism, Binding Affinities, and KRI Values, for Human CB_1 Receptor Antagonists with Various "Left Arm" R^1 Substitutions

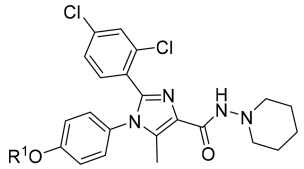

code	R^1	[^{35}S]GTPγS binding pIC_{50} ± SD or SEM (mean IC_{50} in nM)[a]	pK_i[b] ± SEM (mean K_i in nM)	KRI[c]
8a	$-CH_2CH_2CF_3$	8.3 ± 0.1 (5.6)[d]	9.1 ± 0.2 (1.26)	0.90 (0.90, 0.89)
8b	$-CH_2CH_2CH_2F$	8.2 ± 0.01 (6.0)[d]	10 ± 0.2 (0.34)	1.09 (1.34, 0.84)
9	$-CH_2Ph$	7.7 ± 0.1 (18)[d]	8.2 ± 0.1 (6.28)	0.90 ± 0.20
11a	$-CH_2CH_2CH_2CF_3$	8.9 ± 0.1 (1.2)	9.7 ± 0.1 (0.32)	0.80 (0.85, 0.75)
11b	$-SO_2CH_2CH_2CH_3$	8.7 ± 0.03 (1.8)[d]	9.6 ± 0.1 (0.28)	0.59 ± 0.06
11c	$-SO_2CH_2CH_2CH_2F$	8.5 ± 0.2 (3.1)[d]	9.5 ± 0.2 (0.32)	0.88 (1.00, 0.75)
11d	$-SO_2CH_2CH_2CF_3$	9.0 ± 0.03 (1.1)	9.9 ± 0.1 (0.11)	1.02 (1.08, 0.96)
11e	$-SO_2CH_2CH_2CH_2CH_3$	8.9 ± 0.05 (1.3)[d]	9.9 ± 0.1 (0.18)	0.77 ± 0.25
11f	$-SO_2CH_2CH_2CH_2CF_3$	8.9 ± 0.1 (1.2)	10 ± 0.2 (0.062)	0.93 (0.89, 0.97)
11g	$-SO_2CH_2CH_2CH(CH_3)_2$	8.9 ± 0.1 (1.3)	9.7 ± 0.1 (0.20)	1.02 (1.06, 0.97)
11h	$-SO_2CH_2CH_2C(CH_3)_3$	8.7 ± 0.1 (2.4)	9.3 ± 0.1 (0.60)	0.73 (0.68, 0.78)

[a] pIC_{50} ± SD (n = 2) or SEM ($n \geq 3$), obtained from [^{35}S]GTPγS binding on recombinant human CB_1 receptors stably expressed on HEK-293 cell membranes. [b] pK_i ± SEM (n = 3), obtained from radioligand binding assays with [^{3}H]CP55940 on recombinant human CB_1 receptors stably expressed on CHO cell membranes. [c] KRI ± SEM (n = 3) or KRI (n1, n2) (n = 2), obtained from dual-point competition association assays with [^{3}H]CP55940 on recombinant human CB1 receptors stably expressed on CHO cell membranes. [d] n = 2.

Scheme 2. Synthesis of Antagonists 14a–14h, 19, (±)-22, (±)-25, and 28[a]

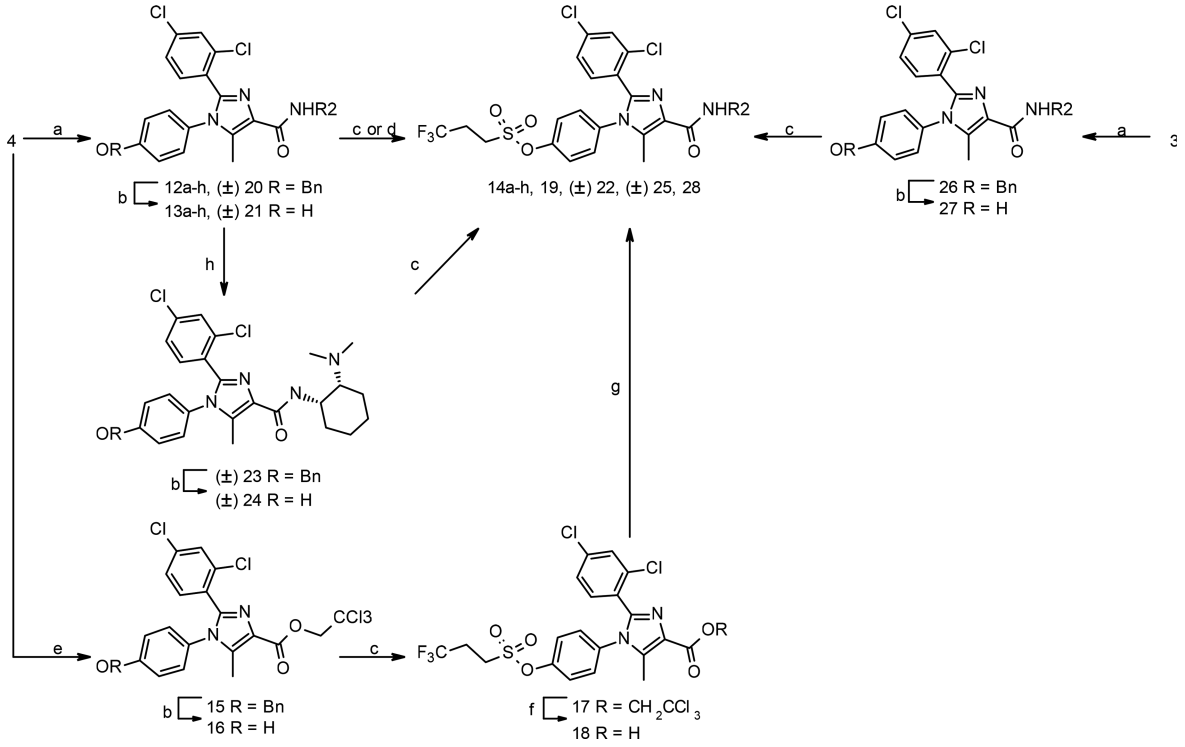

[a] Reagents and conditions: (a) (i) $SOCl_2$, reflux or $(COCl)_2$, DMF cat., CH_2Cl_2, rt, (ii) R^2-NH_2, NEt_3, CH_2Cl_2, 17–98% (2 steps), or 2-amino-5-trifluoromethylpyridine, Me_3Al, CH_2Cl_2, rt to 45 °C, 16 h, 64%; (b) $BF_3{\cdot}OEt_2$, Me_2S, CH_2Cl_2, rt, or HBr, AcOH, rt, 20–97%; (c) Et_3N, $F_3CCH_2CH_2SO_2Cl$, CH_2Cl_2, −78 °C, 25–97%; (d) (i) TBDMSCl, Et_3N, CH_2Cl_2, rt, 22 h, (ii) Boc_2O, THF, rt, 4 h, 70% (4 steps, a, b, d i, and d ii), (iii) TBAF, THF, rt, 90 min, (iv) $F_3CCH_2CH_2SO_2Cl$, Et_3N, CH_2Cl_2, −78 °C, 3 h, (v) $SOCl_2$, MeOH, 0 °C to rt, 1 h, 56% (3 steps, d iii., d iv, and d v); (e) (i) $(COCl)_2$, DMF cat., CH_2Cl_2, rt, 2 h, (ii) Cl_3CCH_2OH, NEt_3, CH_2Cl_2, rt, 3 h, 95% (2 steps, e, b); (f) Zn, AcOH, 3 h; (g) (i) $(COCl)_2$, DMF cat., CH_2Cl_2, rt, 2 h, (ii) 4-aminocyclohexanol, NaOH, H_2O:CH_2Cl_2 2:1, rt, 2 h, 54% (2 steps, f, g); (h) CH_2O, $NaBH_4$, $NaBH_3CN$, CH_3CN, H_2O, AcOH, rt, 48 h, 32%. Corresponding R^2 substitutions are listed in Table 2.

cyclization sequence, the core-imidazole **3** was obtained. Afterward, either saponification of the ethyl ester or acidic hydrolysis of the benzyl ether of **3** led to intermediates **4** and **5**, respectively. Subsequently, Mitsunobu reaction on intermediate **5** yielded mono- and trifluoropropyl ether derivatives **6a** and **6b**. After saponification of the ethyl esters of **6a** and **6b**, the corresponding

DOI: 10.1021/acs.jmedchem.7b00861
J. Med. Chem. 2017, 60, 9545–9564

Table 2. In Vitro Pharmacology Data Including Conventional Antagonism, Binding Affinity, and KRI Values for Human CB_1 Receptor Antagonists with Various "Right Arm" R^2 Substituents

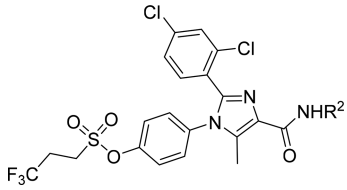

Code	R^2	[^{35}S]GTPγS binding pIC_{50} ± SD or SEM (mean IC_{50} in nM) [a]	pK_i [b] ± SEM (mean K_i in nM)	KRI [c]
11d	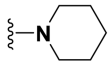	9.0 ± 0.03 (1.1)	9.9 ± 0.1 (0.11)	1.02 (1.08;0.96)
14a (±)	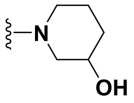	8.6 ± 0.1 (2.7) [d]	9.6 ± 0.1 (0.27)	0.71 ± 0.17
14b (±) *trans*	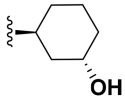	8.9 ± 0.04 (1.1)	10 ± 0.04 (0.10)	0.89 ± 0.12
14c (-) *trans*	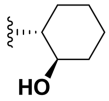	8.8 ± 0.2 (1.7) [d]	9.7 ± 0.2 (0.30)	0.74 ± 0.15
14d (+) *cis*	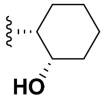	8.8 ± 0.03 (1.8)	11 ± 0.1 (0.027)	1.06 (1.09;1.02)
19 cis : trans (0.3:1)	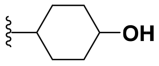	8.4 ± 0.01 (3.8) [d]	9.4 ± 0.1 (0.37)	0.88 ± 0.17
22 (±) *cis*	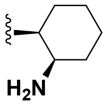	8.2 ± 0.1 (7.1)	9.5 ± 0.2 (0.52)	0.79 (0.65;0.93)
25 (±)*cis*	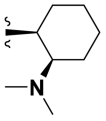	7.1 ± 0.1 (83) [d]	8.6 ± 0.2 (3.3)	0.74 (0.74;0.73)
14e	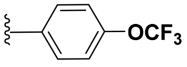	9.2 ± 0.1 (0.66) [d]	9.3 ± 0.4 (0.22)	1.29 ± 0.35
14f	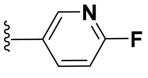	8.9 ± 0.01 (1.2) [d]	10 ± 0.4 (0.13)	0.70 (0.61;0.79)
14g	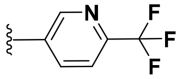	8.7 ± 0.1 (2.2) [d]	9.5 ± 0.2 (0.31)	1.12 ± 0.35
14h	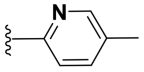	8.8 ± 0.03 (1.7)	9.9 ± 0.1 (0.14)	0.92 ± 0.16
28	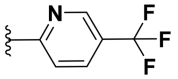	9.2 ± 0.06 (0.61)	9.9 ± 0.1 (0.19)	1.39 ± 0.34

[a] pIC_{50} ± SD (n = 2) or SEM ($n \geq 3$), obtained from [^{35}S]GTPγS binding on recombinant human CB_1 receptors stably expressed on HEK-293 cell membranes. [b] pK_i ± SEM (n = 3), obtained from radioligand binding assays with [^{3}H]CP55940 on recombinant human CB_1 receptors stably

DOI: 10.1021/acs.jmedchem.7b00861
J. Med. Chem. 2017, 60, 9545−9564

Table 2. continued

expressed on CHO cell membranes. [c]KRI ± SEM (n = 3) or KRI (n_1, n_2) (n = 2), obtained from dual-point competition association assays with [^{3}H]CP55940 on recombinant human CB_1 receptors stably expressed on CHO cell membranes. [d]n = 2.

carboxylic acids (**7a** and **7b**) were transformed to acid chlorides and reacted with piperidin-1-amine to yield the corresponding amides (**8a** and **8b**). Alternatively, the rest of the series was produced from intermediate **4** by first introducing the piperidin-1-amide. Lewis acid-catalyzed cleavage of benzyl ether **9** followed by substitution of the released alcohol **10** with various alkyl halides gave the corresponding ethers **11a−11h**, completing the "left arm" series of antagonists (Table 1).

The synthesis of the "right arm" series of antagonists was started from intermediate **4** (Scheme 2). Using various amines and the aforementioned acid chloride introduction/amide formation sequence, amides **12a−12h** were obtained as well as racemic (±)-**20**. Deprotection of the aromatic alcohol on **12a−12h** and subsequent sulfonylation using 3,3,3-trifluoropropane-1-sulfonyl chloride gave compounds **14a−14h**. After deprotection of racemic (±)-**20** however, it was found that direct substitution was not possible, therefore a series of protecting group manipulations was executed on (±)-**21** to end up with (±)-**22**. Toward (±)-**25**, (±)-**20** was first dimethylated and subsequently debenzylated and sulfonylated, giving (±)-**25**. Exploring alternative synthesis routes, compound **19** was synthesized, with a few extra steps, by first esterifying **4** with 2,2,2-trichloroethanol, followed by deprotection of the aromatic alcohol. Sulfonylation of the released alcohol, saponification of the trichloroethylester, acid chloride formation, and subsequent amide formation gave **19**. To obtain trifluoromethylpyridine derivative **28**, conventional methods as described for the industrial production of rimonabant were applied,[35] starting with the direct amidation of ethyl ether **3** followed by debenzylation and sulfonylation.

Biology. All 1,2-diarylimidazol-4-carboxamide derivatives were evaluated as antagonists in an in vitro [^{35}S]GTPγS binding assay on HEK-293 cell membrane fractions overexpressing the human CB_1 receptor. We also determined the functional activity of nine representative antagonists on the human CB_2 receptor. The data in Table 1 and Supporting Information, Table S1 shows that all compounds tested had higher functional activity for the human CB_1 receptor over the human CB_2 receptor, with approximately 110−570-fold selectivity.

Likewise, they were also tested in a [^{3}H]CP55940 radioligand displacement assay on membrane fractions of CHO cells overexpressing the recombinant human CB_1 receptor. These results are reported in Tables 1 and 2. We found that, although using different cellular background and assay systems, there is a significant correlation (r^2 = 0.49, P = 0.0001) between the affinity (pK_i) values from the radioligand binding assay and the potencies (pIC_{50}) determined in the [^{35}S]GTPγS binding assay (Figure 2). We subsequently determined the binding kinetics of the 1,2-diarylimidazol-4-carboxamide derivatives in a competition association assay with [^{3}H]CP55940 as the probe after a validation step.

[^{3}H]CP55940 Binding Kinetic Assay. Receptor association and dissociation rate constants of [^{3}H]CP55940 were directly determined in classic radioligand association and dissociation experiments at 30 °C. The binding of [^{3}H]CP55940 approached equilibrium after approximately 25 min (Figure 3), yielding a k_{on} (k_1) value of (1.4 ± 0.08) × 10^6 M^{-1} s^{-1}. Binding of the radioligand was reversible after the addition of rimonabant (10 μM), although the dissociation was rather slow. Even 240 min after the addition of rimonabant, residual receptor binding (~15%) of

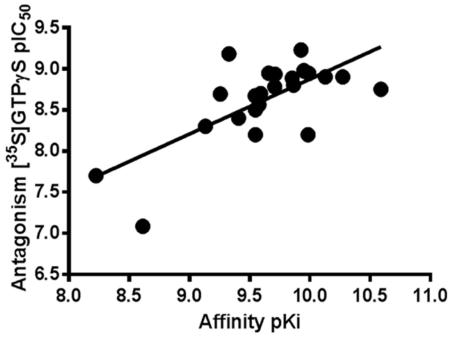

Figure 2. Correlation between the affinities/potencies of the CB_1 receptor antagonists measured in a radioligand binding assay (X-axis) and in a GTPγS binding assay (Y-axis) (r^2 = 0.49, P = 0.0001). Data taken from Tables 1 and 2

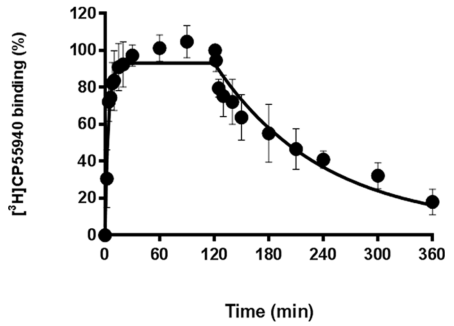

Figure 3. Association and dissociation profile of [^{3}H]CP55940 (2.9 nM) at recombinant hCB_1 receptors stably expressed on CHO cell membranes at 30 °C. After 120 min of association, unlabeled rimonabant (10 μM) was added to initiate the dissociation. Association data was fitted in Prism 6 using one-phase exponential association (n = 3, combined and normalized). Dissociation data was fitted using one-phase exponential decay (n = 4, combined and normalized). Data are shown as mean ± SEM from at least three separate experiments each performed in duplicate.

[^{3}H]CP55940 was observed. The dissociation rate constant, k_{off} (k_2), of [^{3}H]CP55940 from the hCB_1 receptor was (1.5 ± 0.2) × 10^{-4} s^{-1}. The kinetic K_D value (k_{off}/k_{on}) of [^{3}H]CP55940 was 0.12 ± 0.03 nM (Table 3). The residence time (RT) of [^{3}H]CP55940 was calculated as 114 ± 16 min.

Validation of the [^{3}H]CP55940 Competition Association Assay for Human CB_1 Receptor. With the k_{on} (k_1) and k_{off} (k_2) values of [^{3}H]CP55940 binding established from classical association and dissociation experiments, k_{on} (k_3) and k_{off} (k_4) of unlabeled CP55940 were determined by fitting the values based on the mathematical model as described in the Experimental Section.[36] In this validation experiment, we tested three different concentrations of unlabeled CP55940, corresponding to IC_{25}, IC_{50}, and IC_{75} (Figure 4a). Values for k_{on} and k_{off} determined by this competition association method were (1.2 ± 0.1) × 10^6 M^{-1} s^{-1} and (6.5 ± 1.0) × 10^{-4} s^{-1}, respectively. The k_{on} value was in good agreement with the k_{on} (k_1) value determined in the classical association experiment (Table 3). The k_{off} value obtained by this method was also similar to that found in the classical kinetic dissociation experiments with [^{3}H]CP55940, with just a 4-fold

DOI: 10.1021/acs.jmedchem.7b00861
J. Med. Chem. 2017, 60, 9545−9564

Table 3. Comparison of Equilibrium Binding and Kinetic Parameters of CP55940 Determined Using Different Methods[a]

assay	K_i or K_D (nM)	k_{on} (M^{-1} s^{-1})	k_{off} (s^{-1})
displacement[b]	0.56 ± 0.04	NA[c]	NA
association and dissociation[d]	0.12 ± 0.03	$(1.4 \pm 0.08) \times 10^6$	$(1.5 \pm 0.2) \times 10^{-4}$
competition association[e]	0.54 ± 0.10	$(1.2 \pm 0.1) \times 10^6$	$(6.5 \pm 1.0) \times 10^{-4}$

[a]Data are presented as means ± standard error of the mean (SEM) of at least three independent experiments performed in duplicate. [b]Equilibrium displacement of [^{3}H]CP55940 from hCB_1 receptor at 30 °C. [c]Not applicable. [d]Classic association and dissociation parameters of [^{3}H]CP55940 measured in standard kinetic assays at 30 °C. [e]Association and dissociation parameters of CP55940 measured in competition association assays at 30 °C.

difference between the values (Table 3). To confirm the robustness of the assay with unlabeled human CB_1 receptor antagonists, an experiment was performed using rimonabant (Figure 4b,

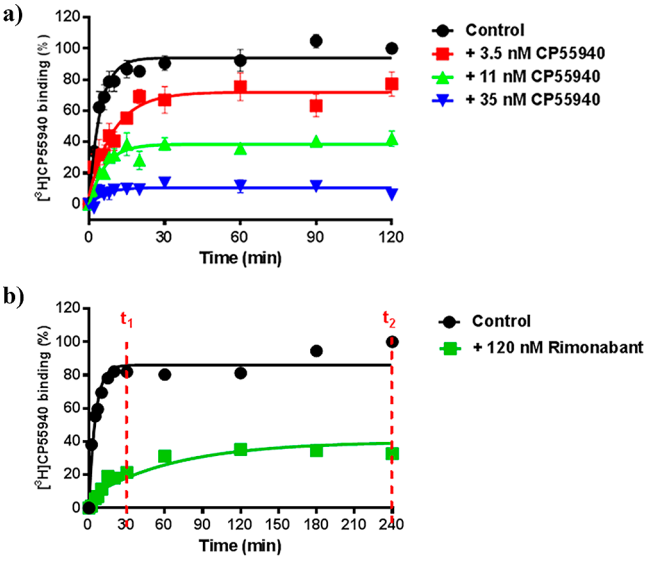

Figure 4. (a) Competition association experiments with [^{3}H]CP55940 binding to recombinant hCB_1 receptors stably expressed on CHO cell membranes (30 °C) in the absence or presence of 3.5, 11, and 35 nM of unlabeled CP55940 (n = 3, combined and normalized). (b) Competition association experiments with [^{3}H]CP55940 binding to recombinant hCB_1 receptors stably expressed on CHO cell membranes (30 °C) in the absence or presence of 120 nM of unlabeled Rimonabant (n = 6, representative graph). t_1 is the radioligand binding at 30 min, while t_2 is the radioligand binding at 240 min.

Table 4). The k_{on} and k_{off} values determined by this competition association method were $(2.3 \pm 0.3) \times 10^5$ M^{-1} s^{-1} and $(1.4 \pm 0.2) \times 10^{-3}$ s^{-1}, respectively, demonstrating that rimonabant behaves as a short residence time antagonist (14 ± 2.0 min), in good agreement with findings reported earlier.[37,38]

Table 4. Kinetic Parameters (k_{on}, k_{off}, and RT) of Selected Human CB_1 Receptor Antagonists

code	k_{on}[a] (M^{-1} s^{-1})	k_{off}[b] (s^{-1})	RT[c] (min)
11b	$(3.0 \pm 0.5) \times 10^5$	$(2.2 \pm 0.2) \times 10^{-4}$	78 ± 5
14f	$(7.2 \pm 3.2) \times 10^5$	$(2.7 \pm 0.5) \times 10^{-4}$	62 ± 10
28	$(3.5 \pm 0.7) \times 10^5$	$(7.8 \pm 0.3) \times 10^{-5}$	260 ± 56
rimonabant	$(2.3 \pm 0.3) \times 10^5$	$(1.4 \pm 0.2) \times 10^{-3}$	14 ± 2.0

[a]k_{on} ± SEM (n = 3), obtained from competition association assays with [^{3}H]CP55940 on recombinant human CB_1 receptors stably expressed on CHO cell membranes. [b]k_{off} ± SEM (n = 3), obtained from competition association assays with [^{3}H]CP55940 on recombinant human CB_1 receptors stably expressed on CHO cell membranes. [c]RT = 1/(60 * k_{off}); RT is expressed in min, whereas k_{off} is expressed in s^{-1}

Screening of hCB_1 Receptor Antagonists Using the Dual-Point Competition Association Assay. The competition association assay described above is quite laborious and time-consuming. Therefore, a so-called "dual-point competition association assay" for the hCB_1 receptor was developed according to the concept that we had previously established for the adenosine A_1 receptor.[32] To this end, [^{3}H]CP55940 and unlabeled antagonists were coincubated at concentrations equal to, or 2−3-fold higher than their K_i/IC_{50} values, which had been determined in the [^{3}H]CP55940 displacement assay. The so-called kinetic rate index (KRI) was calculated by dividing the specific radioligand binding at 30 min (t_1) by the binding at 240 min (t_2). Antagonists with a KRI value larger than 1 indicate a slower dissociation rate and thus a longer RT than [^{3}H]CP55940 and vice versa. Furthermore, it was observed that the KRI values of the hCB_1 receptor antagonists had no obvious correlation with their affinities (Figure 5a).

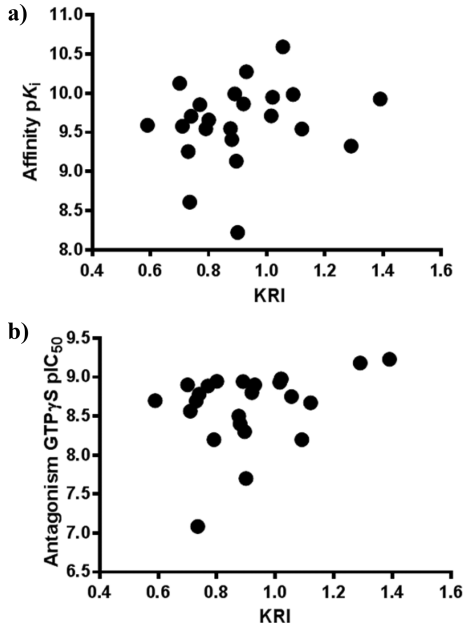

Figure 5. (a) Negative logarithm of the affinities of the hCB_1 receptor antagonists used in this study had no obvious linear correlation with their KRI values (r^2 = 0.04, P = 0.33). (b) Negative logarithm of [^{35}S]GTPγS IC_{50} values of the hCB_1 receptor antagonists in this study had no obvious linear correlation with their KRI values (r^2 = 0.12, P = 0.10).

Structure−Affinity Relationships (SARs) versus Structure−Kinetic Relationships (SKRs). The 1,2-diarylimidazol-4-carboxamide derivatives are rimonabant bioisosteres, in which the 2,4-dichlorophenyl, amide, aryl, and methyl moieties are maintained on an alternative heterocyclic diazo core (Figure 1a,d). The derivatives included in this study differ in their substituents at the

DOI: 10.1021/acs.jmedchem.7b00861
J. Med. Chem. 2017, 60, 9545−9564

R^1 and R^2 positions, which are at the "left" and "right" arms of the scaffold, respectively (Figure 1d).

We were conscious that compound polarity may influence the activity parameters being studied, so polarity was determined by both calculated and experimental methods. Calculated methods included polar surface area (PSA),[39] ACDlogD7.4 with pK_a correction,[40] and AZlogD7.4,[41] which were supplemented with experimentally determined Log *D* values. A PSA of 90 Å^2 has been described as a threshold value below which penetration of the blood−brain barrier is more likely and thus serves as an indicator for potential to have CNS activity.[42] The calculated PSA values (Supporting Information, Tables S2 and S3) of most of the compounds in this study were above 90 Å^2, suggesting that they would have low blood−brain barrier penetration and be better suited for peripheral antagonism of the hCB_1 receptor. We observed that neither affinities nor KRI values of the CB_1 receptor antagonists in this study had any obvious linear correlation with their lipophilicity or PSA values (Supporting Information, Figures S1 and S2).

"Left Arm" Optimization. Fixing the right arm as a piperidine moiety, as in rimonabant, various ethers with different carbon chain lengths were introduced on the left arm (Table 1). Extension of the trifluoromethylalkyl chain from three carbons (**8a**, 1.26 nM) to four atoms (**11a**, 0.32 nM) increased affinity by about 4-fold. Reducing the level of fluorination on the terminal carbon of the linear ether side chain from three atoms (**8a**, 1.26 nM) to one atom (**8b**, 0.34 nM) also increased the affinity. By contrast, the analogue possessing a benzyl substituent on the left arm (**9**, 6.28 nM) displayed the weakest affinity of the analogues studied. The aforementioned modifications did not seem to have a drastic effect on KRI, with all compounds giving values around unity (0.80−1.09). As part of a strategy to increase PSA, a sulfonyl-containing side chain was introduced. The ligand bearing an *n*-propyl-sulfonyl moiety (**11b**) displayed a good affinity of 0.28 nM and a rather low KRI value of 0.59. Monofluorinating the terminal position led to no change in affinity (**11c**, 0.32 nM). In contrast to the ether substituents, trifluorination resulted in an almost 3-fold increase (**11d**, 0.11 nM) relative to the monofluoro analogue. A slight increase in affinity was observed when the linear sulfonyl side chain was extended from three carbon atoms (**11b**, 0.28 nM) to four (**11e**, 0.18 nM). Combination of this chain length with trifluoro-substitution, to give the side chain found in the CB_1 receptor agonist (−)-(*R*)-3-(2-hydroxymethylindanyl-4-oxy)phenyl-4,4,4-trifluoro-1-sulfonate (BAY 38-7271),[43,44] led to a very potent antagonist of the human CB_1 receptor (**11f**, 62 pM). Branching the chain from *n*-butyl to *i*-pentyl did not change the affinity (**11g** vs **11e**) while introducing an additional methyl group led to a decrease in affinity (**11h**, *t*-hex chain, 0.60 nM). None of these ligands had a KRI value higher than 1, indicating their dissociation from the hCB_1 receptor was faster than CP55940. The analogue with the lowest KRI value (**11b**, 0.59) was selected for full-curve measurement (Figure 6, Table 4). As expected, its residence time (78 min) was shorter than that of CP55940 (114 min, see above) (Table 4). This result also serves as evidence that a KRI value seems to reliably reflect the corresponding dissociation rate constant.

All the linear side chain antagonists had high affinities in the nanomolar to subnanomolar range, with **11f** (60 pM) as the most potent derivative. However, from the perspective of drug−target kinetic studies, despite giving a range of KRIs (0.59−1.09), none of these antagonists showed a KRI value significantly higher than 1, suggesting that none had longer residence times than CP55940.

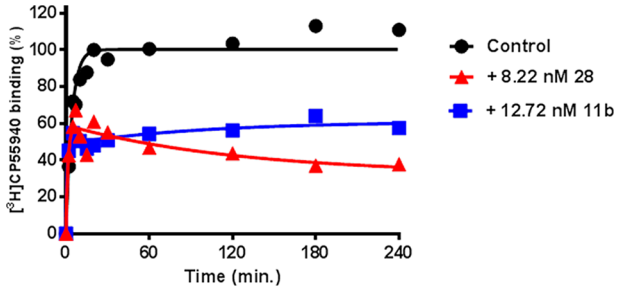

Figure 6. Competition association experiments with [^{3}H]CP55940 binding to recombinant hCB_1 receptors stably expressed on CHO cell membranes (30 °C) in the absence or presence of unlabeled long residence time compound **28** (8.22 nM, red, representative curve) or short residence time compound **11b** (12.72 nM, blue, representative curve). Data are shown as mean values from one representative experiment. At least three separate experiments each performed in duplicate.

"Right Arm" Optimization. To explore the "right arm" of the 1,2-diarylimidazol-4-carboxamides, we chose to fix the "left arm" as a trifluoropropyl sulfonyl moiety (**11d**) because this group delivered high affinity (0.11 nM) and demonstrated a residence time similar to CP55940 (KRI = 1.02, Table 1). Introducing a hydroxyl at the 3-position of the piperidine ring yielded a ligand with lower affinity and KRI value (**14a**, K_i = 0.27 nM, KRI = 0.71) than **11d** (Table 2).

Efforts then focused on a series of ligands bearing cyclohexyl substituents instead of a piperidine. A carbocyclic analogue of **14a**, bearing a *trans*-hydroxyl on the 3-position of the cyclohexyl ring **14b** (racemic), delivered an approximately 3-fold improvement in affinity and a slightly larger KRI value relative to the piperidine **14a** (Table 2). Moving the hydroxyl to the 4-position gave 4-hydroxycyclohexyl analogue (**19**) as a mixture of cis and trans diastereoisomers in a ratio of 0.3:1 and resulted in an approximately 4-fold reduction in affinity (0.37 nM), while the KRI was unchanged (0.88); having a mixture does not allow any further conclusions, though. Interestingly, the *cis*- and *trans*-2-hydroxycyclohexyl antagonists (**14d** and **14c**, respectively) showed a substantial 10-fold difference in affinity, while their KRI values were quite similar. The more potent *cis*-isomer (**14d**, (+)) displayed an affinity of 27 pM and a KRI value close to unity. Switching the 2-substituent of the cyclohexane ring to an amine was detrimental, resulting in ligands with lower affinities. However, it is of note that the unsubstituted *cis*-amino group (**22**, (±), 0.52 nM) was less detrimental to affinity than a *cis*-dimethylamino substituent (**25**, (±), 3.3 nM), while the dissociation rates were very similar, as judged by their KRI values (Table 2). At this stage, on the basis of affinity alone, **14d** with an affinity of 27 pM seems an even better lead than **11f** with an affinity of 62 pM.

Last but not least, we found that by introducing an aromatic moiety, the compounds retain affinity in the subnanomolar range and, more importantly, their kinetic profiles were rather diverse. The analogue which bears a 4-trifluoromethoxyphenyl substituent (**14e**) showed high affinity (0.22 nM) and its KRI value was one of the highest measured (Table 2). Introduction of a pyridine moiety was then studied. The 3-pyridyl analogues **14f** and **14g**, bearing a 6-fluoro or trifluoromethyl group, respectively, showed similar affinities (0.13 vs 0.31 nM, respectively), although the latter had a much higher KRI value (1.12 vs 0.70, respectively). This effect on KRI was increased further when the position of the nitrogen atom in the ring was switched to give the 5-substituted 2-pyridyl analogue (**28**, KRI = 1.39), which displayed the highest KRI value of all the compounds presented

DOI: 10.1021/acs.jmedchem.7b00861
J. Med. Chem. 2017, 60, 9545−9564

in this study. Finally, defluorinating this latter compound did not change the affinity but gave rise to a marked reduction in KRI (**14h**, K_i = 0.14 nM, KRI = 0.92).

The compounds with high (**28**) and low (**11b** and **14f**) KRI values were tested in a full competition association assay to determine their association and dissociation rate constants (Figure 6 and Table 4). According to the full curves, the compound with KRI > 1 (**28**) displayed an "overshoot" in the competition association curve, indicating its slow dissociation and yielding the longer residence time of 260 min, as compared to 114 min of the radioligand. By contrast, the compounds with KRI < 1 produced gradually ascending curves, suggesting faster dissociation and consequently shorter residence times of 78 min (**11b**) and 62 min (**14f**) (Figure 6, Table 4). Additionally, we determined their affinities on the human CB_2 receptor. From Table 1 and Supporting Information, Table S1, they show that they all had higher affinity for the human CB_1 receptor, where approximately 12−125-fold selectivity over human CB_2 receptors was observed.

Functional Assays. As mentioned above, the antagonism in the [^{35}S]GTPγS binding assay compares quite well with the affinities derived from the [^{3}H]CP55940 displacement studies (Figure 2), while the KRI values of the compounds did not show any meaningful correlation with the pIC_{50} values from the GTPγS binding assay (Figure 5b). Because **28** showed slow dissociation, we decided to study this compound further in a more elaborate [^{35}S]GTPγS binding experiment in which its functional activity in the inhibition of CP55940 action was characterized and compared with rimonabant. Pretreatment of CHOK1 hCB_1 receptor membranes with rimonabant for 1 h, prior to stimulation by the CB_1 receptor agonist CP55940 for 30 min, induced surmountable antagonism (a rightward shift of the agonist curve with little suppression of the maximum effect) as reported before.[45] In the case of **28**, insurmountable antagonism was observed; the agonist concentration−effect curve was shifted to the right with a concomitant decrease (~50%) in its maximal response (Figure 7). In both cases, inverse agonism by the compounds alone (in the absence of CP55940) was also apparent (negative values at *Y*-axis in Figure 7).

Computational Studies. Finally, we investigated the ligand−receptor interactions using the recently disclosed X-ray crystal structure of hCB_1 in complex with **29** [4-(4-(1-(2,4-dichlorophenyl)-4-methyl-3-(piperidin-1-ylcarbamoyl)-1*H*-pyrazol-5-yl)phenyl)but-3-ynyl nitrate, AM6538], crystal structure code PDB 5TGZ.[32] By docking **28** into the hCB_1 receptor, it can be seen that, like **29**, it lies quite deep in the binding pocket of hCB_1 in the docked pose, immediately above the conserved Trp356$^{6.48}$ (Figures 8a,b). The main scaffold of the imidazole core and the 2,4-dichlorophenyl ring forms a π−π interaction with the side chains of Phe102$^{N\text{-term}}$ and Phe170$^{2.57}$, respectively (Figure 8b). Unsurprisingly, and consistent with the SAR reported in Table 1, the "left arm" of our ligand docks into the same place as "Arm 2" of **29** in the crystal structure. This "left arm" extends into a long, narrow, and highly lipophilic channel formed by helices III, V, VI, and ECL2 (Figure 8a). By contrast, the "right arm" of our ligands, which resemble "Arm 3" of **29**, dock into an open cavity formed by various hydrophobic amino acid residues,[33] irrespective of whether a cyclohexyl, piperidine, or pyridine moiety is present. In the case of a pyridine moiety (**14e−14h** and **28**), the crystal structure suggests that there may be a π−π stacking interaction with His178$^{2.65}$. Further support for the docked pose of **28** comes from the higher resolution X-ray structure of taranabant bound to hCB1 (PDB 5U09)[34] because both compounds share a trifluoromethylpyridine moiety on their "right arm".

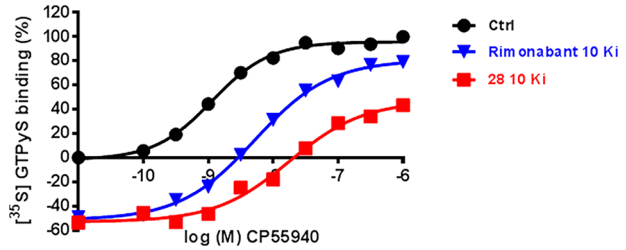

Figure 7. CP55940-stimulated [^{35}S]GTPγS binding to recombinant hCB_1 receptors stably expressed on CHO cell membranes (25 °C) in the absence (black, representative curve) or presence of long-residence-time compound **28** (red, representative curve) or rimonabant (blue, representative curve). Compound **28** or rimonabant was preincubated with the membranes for 1 h prior to the challenge of agonist. [^{35}S]GTPγS was subsequently added and incubated for another 0.5 h. Plates were then filtered and the radioactivity counted. Curves were fitted to a four parameter logistic dose−response equation. Data were normalized according to the maximal response (100%) produced by CP55940. At least three separate experiments each performed in duplicate.

Using the crystal structure of the hCB_1−**29** complex, we performed WaterMap calculations to try and understand the differences in residence times observed for the ligands studied, with the hypothesis that unfavorable hydration might provide an explanation.[46−48] We focused on the pyridine ring substituents on the "right arm", and ligands **14f** and **28** in particular, because of their similar binding affinities but differing residence times. The smaller of the two ligands (**14f**, −F substitution, relatively short RT) was docked into the hCB_1 receptor, and a WaterMap was calculated for the complex. Around the F substituent, we found unstable water molecules (41, 69, 72, 81, and 88 in Figure 8c); these water molecules are coined "unhappy" waters.[49] By contrast, ligand **28** was able to displace these water molecules with its larger $-CF_3$ substituent, a process which might raise the energy of the transition state for dissociation. We postulate that this destabilization of the transition state may contribute to the prolonged residence time observed with this compound.

CONCLUSIONS

We have demonstrated that, in addition to affinity, knowledge of binding kinetics is useful for selecting and developing new hCB_1 receptor antagonists in the early phases of drug discovery. In the specific case of the hCB_1 receptor, a long residence time compound may be beneficial for a peripherally selective antagonist. We explored SAR and SKR parameters in a series of 1,2-diarylimidazol-4-carboxamide derivatives by examining the influence of substitutions at both "arms" of the molecules.

By introducing more polar linear sulfonyl side chains on the "left arm", affinity could be modulated, however, the KRI values indicative for the compounds' kinetic properties were less than or similar to CP55940. Substitution of the "right arm" maintained or increased affinity, and with the introduction of an aromatic ring system, KRI values >1 were obtained. With a residence time of 260 min, which is substantially longer than CP55940 (114 min) or rimonabant (14 min), 4-(2-(2,4-dichlorophenyl)-5-methyl-4-((5-(trifluoromethyl)pyridin-2-yl)carbamoyl)-1*H*-imidazol-1-yl)-phenyl-3,3,3-trifluoropropane-1-sulfonate (**28**) stood out from the ligands studied. This slowly dissociating hCB_1 receptor antagonist also showed insurmountability in a functional GTPγS binding assay. Using the recently resolved hCB_1 crystal structures, we analyzed the putative interactions of **28** with the receptor, from which we speculate that displacement of "unhappy" water

DOI: 10.1021/acs.jmedchem.7b00861
J. Med. Chem. 2017, 60, 9545−9564

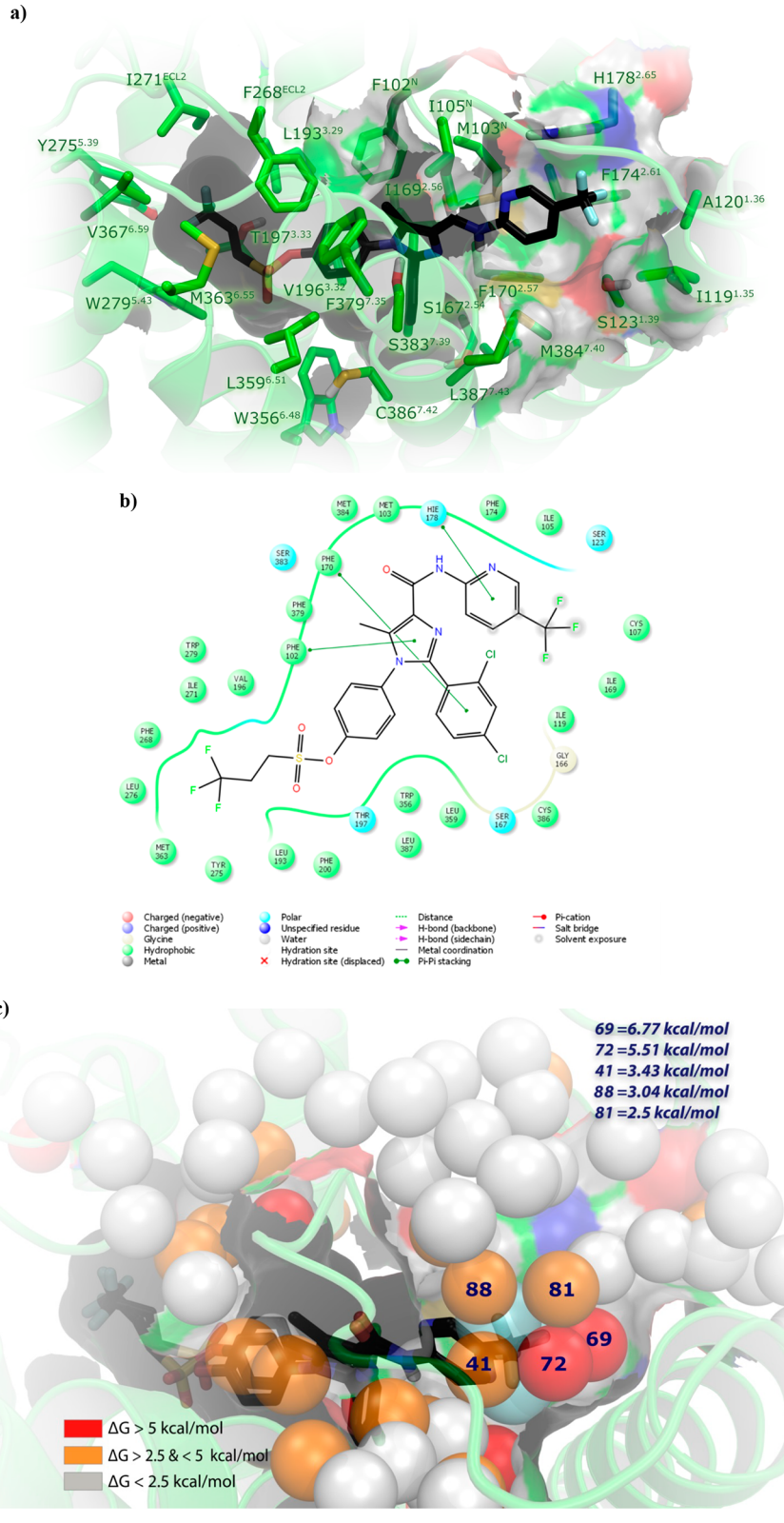

Figure 8. (a) Docking of antagonist **28** into the binding site of the crystal structure of the CB_1 receptor (PDB 5TGZ)[33] co-crystallized with **29** (not shown). Compound **28** is represented by black sticks, and residues within 5 Å of **28** are visualized as green sticks. The protein is represented by green ribbons, and relevant binding site confinements are indicated by white-gray (hydrophobic), red (electronegative), and blue (electropositive) layers. Ligand and residues atoms color code: yellow = sulfur, red = oxygen, blue = nitrogen, cyan = fluorine, white = hydrogen. (b) 2-D interaction map of **28** docking into the CB1 receptor co-crystallized with **29** (PDB 5TGZ),[33] demonstrating $\pi-\pi$ stacking between imidazole core of **28** and $Phe102^{N\text{-term}}$, 2,4-dichlorophenyl ring and $Phe170^{2.57}$, and pyridine and $His178^{2.65}$. (c) Docking of **14f** and **28** into the binding site of the crystal structure of the CB1 receptor co-crystallized with **29** (PDB 5TGZ),[33] showing the overlay of numbered consecutively hydration sites of **14f** (colored spheres; for color code, see below) calculated by WaterMap. Hydration sites shown as red and orange spheres represent "unstable" water molecules. White spheres symbolize "stable" water molecules, which should not be displaced by **14f** or **28**. For the key hydration sites (41, 69, 72, 81, 88) surrounding the −F atom of **14f**, calculated ΔG values (in kcal/mol) with respect to bulk solvent are shown.

DOI: 10.1021/acs.jmedchem.7b00861
J. Med. Chem. 2017, 60, 9545−9564

molecules may provide a plausible explanation for its slow dissociation. Therefore, compound **28**, or derivatives with similar characteristics, may be a useful tool to test whether prolonged blockade of the (peripheral) hCB_1 receptor has a beneficial effect on CB_1 receptor related disorders such as obesity.

EXPERIMENTAL SECTION

Chemistry. All solvents and reagents were purchased from commercial sources and were of analytical grade. Demineralized water is simply referred to as water or H_2O, as was used in all cases unless stated otherwise (i.e., brine). Thin-layer chromatography (TLC) was routinely consulted to monitor the progress of reactions, using aluminum-coated Merck silica gel F_{254} plates. Purification was performed on a semipreparative high performance liquid chromatography (HPLC) with a mass triggered fraction collector, a Shimadzu QP 8000 single quadrupole mass spectrometer equipped with a 19 mm × 100 mm C8 column. The mobile phase used was, if nothing else is stated, acetonitrile and buffer (aqueous NH_4OAc (0.1 M): acetonitrile 95:5). For isolation of isomers, a Kromasil CN E9344 (250 mm × 20 mm i.d.) column was used. A mixture of heptane/ethyl acetate/diethylamine 95:5:0.1 was used as mobile phase (1 mL/min). Fraction collection was guided using a UV detector (330 nm). Analytical purity of the final products was determined by Waters Acquity I-class ultraperformance liquid chromatography (UPLC) consisting of a binary solvent system, ultraviolet (UV) photodiode array (PDA) detector, column temperature control manager, and sample manager modules, coupled with in-line and mass spectrometry detection. The sample was injected onto, and separated by, a Waters Acquity BEH (C18) 1.7 mm (150 mm × 3 mm) UPLC column maintained at 40 °C and eluted with 0.1% ammonium hydroxide in water (A) and acetonitrile (B) at a flow rate of 1 mL/min, using a linear gradient. Initial conditions started at 3% B, which was increased to 97% over 1.3 min and maintained for 0.2 min before returning to initial conditions over 0.2 min prior to the next injection. Eluent containing UPLC-separated analytes then flowed via the UV PDA detector scanning between 220 and 320 nm wavelengths at a resolution of 1.2 nm sampling at 40 points/s into a Waters SQD single quadrupole mass spectrometer (MS) fitted with an electrospray source. All MS analyses were acquired for a total run time of 2 min, with mass scanning from 100 to 1000 μ in both positive and negative ion modes alternately, using electrospray ionization (ESI). Typical MS settings included: capillary voltage, 1 kV; cone voltage, 25 V; source temperature, 150 °C; desolvation temperature, 350 °C. The data were acquired via a PC running MassLynx v4.1 in open access mode and processed and reported via OpenLynx software application. For each sample, the purity is determined by integration of the UV absorption chromatogram. All final compounds show a single peak and are at least 95% pure.

^1H NMR measurements were performed on either a Varian Mercury 300 or a Varian Inova 500, operating at ^1H frequencies of 300 and 500 MHz respectively at ambient temperature. Chemical shifts are reported in parts per million (ppm), are designated by δ, and are downfield to the internal standard tetramethylsilane (TMS) in $CDCl_3$. Coupling constants are reported in Hz and are designated as *J*. High-resolution mass spectra were recorded on either a Micromass ZQ single quadrupole or a Micromass LCZ single quadrupole mass spectrometer both equipped with a pneumatically assisted electrospray interface (LC-MS). Melting points were determined on a Reichert melting point microscope and are uncorrected.

*N-(4-(Benzyloxy)phenyl)-2,4-dichlorobenzamidine (**2**).* Compound **1** (5.0 g, 21.2 mmol) was added dropwise to a solution of ethyl magnesium bromide (44.5 mL, 1 M in THF, 44.5 mmol) in dry THF (25 mL) under a nitrogen atmosphere. After stirring for 20 min, a solution of 2,4-dichlorobenzonitrile (3.65 g, 21.2 mmol) in THF (25 mL) was added. The reaction mixture was stirred for 20 h at rt. Water (50 mL) was carefully added. Extraction with EtOAc (2 × 100 mL), drying (Na_2SO_4), filtration, and evaporation to dryness afforded the crude title compound (7.7 g, 98%).

*Ethyl 1-(4-(Benzyloxy)phenyl)-2-(2,4-dichlorophenyl)-5-methyl-1H-imidazole-4-carboxylate (**3**).* To a solution of compound **2** (6.88 g, 18.5 mmol) in THF (50 mL) was added potassium carbonate (2.56 g, 18.5 mmol), and the suspension was stirred for 10 min. Ethyl-3-bromo-2-oxobutanoate (4.65 g, 22.2 mmol) was added dropwise over 1 h, and the mixture was stirred for 66 h at rt. The solution was filtered and evaporated to dryness. The residue was dissolved in AcOH and refluxed for 1 h. The mixture was cooled to rt, water (100 mL) added, and the product extracted with EtOAc (2 × 200 mL). The combined organic phases were washed with saturated aqueous sodium hydrogen carbonate, dried (Na_2SO_4), filtered, and concentrated in vacuo. Flash chromatography (silica, 30−40% EtOAc in hexane) afforded the title compound (5.75 g, 65%) as a pale-yellow solid. ^1H NMR ($CDCl_3$): δ 7.50−7.20 (m, 8H), 7.10−6.90 (m, 4H), 5.10 (s, 2H), 4.50 (q, 2H), 2.5 (s, 3H), 1.5 (t, 3H).

*1-(4-(Benzyloxy)phenyl)-2-(2,4-dichlorophenyl)-5-methyl-1H-imidazole-4-carboxylic Acid (**4**).* To a suspension of compound **3** (3.62 g, 7.5 mmol) in MeOH (60 mL) was added potassium hydroxide (4.05 g, 72 mmol) in water (20 mL) and the reaction mixture heated to reflux. After 2 h the mixture was cooled to rt, acidified to pH ∼ 2 with HCl (1 M), and extracted with ethyl acetate (2 × 200 mL). The combined organic phases were dried (Na_2SO_4), filtered, and concentrated in vacuo to give the crude title compound (3.38 g, 99%).

*Ethyl 2-(2,4-Dichlorophenyl)-1-(4-hydroxyphenyl)-5-methyl-1H-imidazole-4-carboxylate (**5**).* Compound **3** (4.82 g, 10 mmol) was dissolved in HBr (33% in AcOH, 80 mL) and stirred overnight at rt with exclusion of light. The solvents were evaporated and the residue coevaporated with EtOH. The residue was dissolved in EtOH, HCl (4 M in dioxane, 5 mL), and $MgSO_4$ were added, and the resulting mixture heated under reflux for 2.5 h. The reaction mixture was cooled to rt, filtered, and concentrated in vacuo. The residue was dissolved in EtOAc and washed with water basified with triethylamine and then brine. The organic layer was dried over Na_2SO_4 and concentrated in vacuo to give the crude title compound (4.74 g) as a brown, viscous oil of sufficient purity for the next step.

*Ethyl 2-(2,4-Dichlorophenyl)-5-methyl-1-(4-(3,3,3-trifluoropropoxy)phenyl)-1H-imidazole-4-carboxylate (**6a**).* A solution of compound **5** (978 mg, 2.5 mmol), 3,3,3-trifluoro-1-propanol (428 mg, 3.75 mmol), and triphenylphosphine (984 mg, 3.75 mmol) in anhydrous THF (12 mL) were treated with DEAD (40% in toluene, 1.72 mL, 3.75 mmol). The resulting mixture was stirred at rt for 30 h then heated to 50 °C overnight. After cooling to rt, additional 3,3,3-trifluoro-1-propanol (428 mg, 3.75 mmol) and triphenylphosphine (984 mg, 3.75 mmol) were added, followed by di-*tert*-butylazodicarboxylate (863 mg, 3.75 mmol) and the resulting mixture stirred at rt overnight. Again, additional 3,3,3-trifluoro-1-propanol (428 mg, 3.75 mmol) and triphenylphosphine (984 mg, 3.75 mmol) were added, followed by di-*tert*-butyl azodicarboxylate (863 mg, 3.75 mmol), and the resulting mixture was stirred at rt overnight. The mixture was concentrated in vacuo and the residue purified by column chromatography (silica gel, 10−50% EtOAc in hexanes) to yield the title compound (880 mg, 68%) as a yellowish foam of sufficient purity for the next transformation. ^1H NMR (500 MHz, $CDCl_3$) δ 7.22−7.16 (m, 3H), 7.01 (d, J = 8.7 Hz, 2H), 6.83 (d, J = 8.7 Hz, 2H), 4.40 (q, J = 7.1 Hz, 2H), 4.22−4.10 (m, 2H), 2.66−2.54 (m, 2H), 2.40 (s, 3H), 1.40 (t, J = 7.1 Hz, 3H).

*Ethyl 2-(2,4-Dichlorophenyl)-1-(4-(3-fluoropropoxy)phenyl)-5-methyl-1H-imidazole-4-carboxylate (**6b**).* A solution of compound **5** (978 mg, 2.5 mmol), 3-fluoropropan-1-ol (293 mg, 3.75 mmol), and triphenylphosphine (984 mg, 3.75 mmol) in anhydrous THF (9 mL) were treated with DEAD (40% solution in toluene, 1.72 mL, 3.75 mmol). The resulting mixture was stirred at rt overnight. The residue was purified by column chromatography (silica gel, 20−40% EtOAc in hexanes). The product containing fractions were combined and concentrated in vacuo. The residue was dissolved in CH_2Cl_2, then an equal amount of hexane was added. The resulting solid was filtered off, and the filtrate concentrated in vacuo to yield the title compound (1.07 g, 85%) as a colorless foam of ca. 90% purity, which was used in the next transformation without further purification. ^1H NMR (500 MHz, $CDCl_3$) δ 7.35−7.20 (m, 3H), 7.03 (d, J = 8.7 Hz, 2H), 6.87 (d, J = 8.7 Hz, 2H), 4.73−4.60 (m, 2H), 4.44 (q, J = 7.1 Hz, 2H), 4.11−4.07 (m, 2H), 2.44 (s, 3H), 2.24−2.13 (m, 2H), 1.44 (t, J = 7.1 Hz, 3H).

*2-(2,4-Dichlorophenyl)-5-methyl-1-(4-(3,3,3-trifluoropropoxy)-phenyl)-1H-imidazole-4-carboxylic Acid (**7a**).* A stirred solution of

DOI: 10.1021/acs.jmedchem.7b00861
J. Med. Chem. 2017, 60, 9545−9564

compound **6a** (880 mg, 1.72 mmol), in a mixture of THF (15 mL) and EtOH (15 mL), was treated with KOH (1.07 g, 19 mmol), dissolved in water (10 mL), and the resulting mixture stirred at 50 °C. After 3 h 30 min, the reaction mixture was cooled to rt then concentrated in vacuo. The residue was partitioned between CH_2Cl_2 and HCl (1 M) and, after phase separation, the aqueous layer was extracted two more times with CH_2Cl_2. The combined organic extracts were dried over $MgSO_4$ and concentrated in vacuo to give the title compound (714 mg, 90%) as a yellowish foam. ^{1}H NMR (500 MHz, $CDCl_3$) δ 7.32−7.18 (m, 3H), 7.00 (d, J = 8.7 Hz, 2H), 6.85 (d, J = 8.7 Hz, 2H), 4.18−4.14 (m, 2H), 2.66−2.55 (m, 2H), 2.42 (s, 3H).

*2-(2,4-Dichlorophenyl)-1-(4-(3-fluoropropoxy)phenyl)-5-methyl-1H-imidazole-4-carboxylic Acid (**7b**).* A solution of compound **6b** (1.07 g, 2.13 mmol, ca. 90% pure), in a mixture of THF (20 mL) and EtOH (20 mL), was treated with KOH (1.40 g, 25 mmol) dissolved in water (10 mL) and the resulting mixture stirred at 50 °C. After 3 h 30 min, the reaction mixture was cooled to rt then concentrated in vacuo. The residue was partitioned between CH_2Cl_2 and HCl (1 M) and, after phase separation, the aqueous layer extracted with CH_2Cl_2 and twice with EtOAc. The combined organic extracts were dried over $MgSO_4$ and concentrated in vacuo to give the title compound (856 mg, 95%) as a yellowish foam which was sufficiently pure for the next step. ^{1}H NMR (500 MHz, $CDCl_3$) δ 7.35−7.22 (m, 3H), 7.04 (d, J = 8.7 Hz, 2H), 6.88 (d, J = 8.7 Hz, 2H), 4.72−4.60 (m, 2H), 4.12−4.09 (m, 2H), 2.46 (s, 3H), 2.25−2.14 (m, 2H).

*2-(2,4-Dichlorophenyl)-5-methyl-N-(piperidin-1-yl)-1-(4-(3,3,3-trifluoropropoxy)phenyl)-1H-imidazole-4-carboxamide (**8a**).* A solution of compound **7a** (643 mg, 1.4 mmol) in CH_2Cl_2 (10 mL) was treated with oxalyl chloride (200 μL, 2.36 mmol), followed by 10 μL of DMF. The resulting mixture was stirred for 90 min at rt, then concentrated in vacuo. The residue was dried under vacuum as a yellowish foam which was used without further purification. Subsequently, to a mixture of piperidin-1-amine hydrochloride (0.3 mmol) and pyridine (100 μL) in CH_2Cl_2 (1 mL) was added a portion of crude intermediate (2-(2,4-dichlorophenyl)-5-methyl-1-(4-(3,3,3-trifluoropropoxy)phenyl)-1*H*-imidazole-4-carbonyl chloride (96 mg, 0.2 mmol)) in CH_2Cl_2 (1 mL), and the resulting mixture stirred at rt for 2 h 30 min. The reaction mixture was washed with saturated aqueous $NaHCO_3$ (2 mL) and, after phase separation, filtered through a phase separator. The solvents were evaporated and the residue purified by preparative HPLC eluting on a reverse-phase column (5−100% acetonitrile in aqueous NH_4OAc (0.1 M)) to give the title compound (45 mg, 41%) as a colorless solid. ^{1}H NMR (500 MHz, $CDCl_3$) δ 7.90 (s, 1H), 7.35 (d, J = 1.9 Hz, 3H), 7.29 (d, J = 8.3 Hz, 1H), 7.23 (dd, J = 1.9, 8.3 Hz, 1H), 7.03 (d, J = 8.9 Hz, 2H), 6.87 (d, J = 8.9 Hz, 2H), 4.19 (t, J = 6.6 Hz, 2H), 2.94−2.81 (m, 4H), 2.69−2.60 (m, 2H), 2.47 (s, 3H), 1.82−1.73 (m, 4H), 1.49−1.41 (m, 2H). HRMS Calcd for $[C_{25}H_{25}Cl_2F_3N_4O_2 + H]$: 541.1385. Found: 541.1366. HPLC: 100%.

*2-(2,4-Dichlorophenyl)-1-(4-(3-fluoropropoxy)phenyl)-5-methyl-N-(piperidin-1-yl)-1H-imidazole-4-carboxamide (**8b**).* A solution of compound **7b** (732 mg, 1.55 mmol) in CH_2Cl_2 (20 mL) was treated with oxalyl chloride (200 μL, 2.36 mmol), followed by DMF (10 μL). The resulting mixture was stirred for 90 min at rt, then concentrated in vacuo. The residue was dried under vacuum as a yellowish foam which was used without further purification. Subsequently, to a mixture of piperidin-1-amine hydrochloride (0.39 mmol) and pyridine (100 μL) in CH_2Cl_2 (2 mL) was added a portion of crude 2-(2,4-dichlorophenyl)-1-(4-(3-fluoropropoxy)phenyl)-5-methyl-1*H*-imidazole-4-carbonyl chloride (115 mg, 0.26 mmol) in CH_2Cl_2 (2 mL), and the resulting mixture was stirred at rt for 2 h. The reaction mixture was washed with saturated aqueous $NaHCO_3$ (2 mL) and, after phase separation, filtered through a phase separator. The solvents were evaporated and the residue purified by preparative HPLC eluting on a reverse-phase column (5−100% CH_3CN in aqueous NH_4OAc (0.1 M)) to give the title compound (74 mg, 56%) as a colorless solid. ^{1}H NMR (500 MHz, $CDCl_3$) δ 7.90 (s, 1H), 7.35 (d, J = 2.0 Hz, 1H), 7.28 (d, J = 8.2 Hz, 1H), 7.23 (dd, J = 2.0, 8.2 Hz, 1H), 7.01 (d, J = 8.9 Hz, 2H), 6.86 (d, J = 8.9 Hz, 2H), 4.66 (dt, J = 5.7, 47.0 Hz, 2H), 4.09 (t, J = 6.1 Hz, 2H), 2.95−2.82 (m, 4H), 2.47 (s, 3H), 2.25−2.13 (m, 2H), 1.81−1.73 (m, 4H), 1.49−1.40 (m, 2H). HRMS Calcd for $[C_{25}H_{27}Cl_2FN_4O_2 + H]$: 505.1573. Found: 505.1572. HPLC: 100%.

*1-(4-(Benzyloxy)phenyl)-2-(2,4-dichlorophenyl)-5-methyl-N-(piperidin-1-yl)-1H-imidazole-4-carboxamide (**9**).* To a solution of compound **4** (3.38 g, 7.5 mmol) in CH_2Cl_2 (60 mL) were added 3 drops of DMF, followed by oxalyl chloride (1.3 mL, 14.9 mmol). The mixture was refluxed for 2 h, then cooled to rt and evaporated to dryness. The residue was dissolved in CH_2Cl_2 (50 mL) and cooled to 0 °C. Triethylamine (2.1 mL, 14.9 mmol) was added, followed by piperidin-1-amine (0.9 mL, 8.2 mmol), and the mixture stirred at rt for 2 h. Water (300 mL) was added, and the mixture extracted with CH_2Cl_2 (3 × 100 mL). The organic extracts were dried (Na_2SO_4), filtered, and concentrated in vacuo. Flash chromatography (silica, 66−100% EtOAc in hexane) afforded the title compound (2.94 g, 74%) as a white solid. ^{1}H NMR (400 MHz, $CDCl_3$) δ 7.71 (d, J = 8.3 Hz, 1H), 7.42−7.32 (m, 7H), 7.29 (dd, J = 1.9, 8.3 Hz, 1H), 7.24 (d, J = 9.0 Hz, 2H), 6.98 (d, J = 9.0 Hz, 2H), 5.04 (s, 2H), 4.05−3.52 (m, 4H), 2.54 (s, 3H), 2.29−2.16 (m, 4H), 1.78−1.57 (m, 2H). HRMS Calcd for $[C_{29}H_{28}Cl_2N_4O_2 + H]$: 535.1667. Found: 535.1667. HPLC: 96.9%.

*2-(2,4-Dichlorophenyl)-1-(4-hydroxyphenyl)-5-methyl-N-(piperidin-1-yl)-1H-imidazole-4-carboxamide (**10**).* A solution of compound **9** (2.78 g, 5.2 mmol) in CH_2Cl_2 (80 mL) was cooled to 0 °C then treated dropwise with boron tribromide (1 M in CH_2Cl_2, 10.4 mL, 10.4 mmol). The reaction mixture was stirred at rt for 1 h then treated with water (200 mL). The mixture was extracted with EtOAc (3 × 200 mL). The combined organic phases were dried (Na_2SO_4), filtered, and concentrated in vacuo. Flash chromatography (silica, 75−100% EtOAc in hexane) afforded the title compound (1.34 g, 58%) as a white solid. ^{1}H NMR (400 MHz, $CDCl_3$) δ 8.66 (br s, 1H), 7.94 (br s, 1H), 7.31 (d, J = 1.9 Hz, 1H), 7.23 (d, J = 8.3 Hz, 1H), 7.18 (dd, J = 1.9, 8.3 Hz, 1H), 6.92−6.85 (m, 4H), 2.90−2.67 (m, 4H), 2.43 (s, 3H), 1.69−1.56 (m, 4H), 1.43−1.30 (m, 2H).

*2-(2,4-Dichlorophenyl)-5-methyl-N-(piperidin-1-yl)-1-(4-(4,4,4-trifluorobutoxy)-phenyl)-1H-imidazole-4-carboxamide (**11a**).* A suspension of compound **10** (351 mg, 0.79 mmol) and K_2CO_3 (218 mg, 1.58 mmol) in acetone (50 mL) was treated dropwise with 1-iodo-4,4,4-trifluorobutane (376 mg, 1.58 mmol). The reaction mixture was refluxed overnight then cooled, filtered, and concentrated in vacuo. Flash chromatography (silica, hexane:EtOAc 1:2) afforded the title compound (200 mg, 46%) as a white solid. ^{1}H NMR (400 MHz, $CDCl_3$) δ 7.91 (br s, 1H), 7.32 (d, J = 1.9 Hz, 1H), 7.27 (d, J = 8.3 Hz, 1H), 7.21 (dd, J = 2.0, 8.3 Hz, 1H), 7.00 (d, J = 8.9 Hz, 2H), 6.83 (d, J = 8.9 Hz, 2H), 3.99 (t, J = 6.0 Hz, 2H), 3.13−2.67 (m, 4H), 2.45 (s, 3H), 2.38−2.23 (m, 2H), 2.10−2.00 (m, 2H), 1.84−1.71 (m, 4H), 1.50−1.38 (m, 2H). MS m/z 578 (M + Na). HRMS Calcd for $[C_{26}H_{27}Cl_2F_3N_4O_2 + H]$: 555.1541. Found: 555.1504. HPLC: 100%.

*4-(2-(2,4-Dichlorophenyl)-5-methyl-4-(piperidin-1-ylcarbamoyl)-1H-imidazol-1-yl)phenyl propane-1-sulfonate (**11b**).* A solution of compound **10** (320 mg, 0.72 mmol) in CH_2Cl_2 (10 mL) was cooled to 0 °C. Et_3N (100 μL, 0.72 mmol) was added, followed by 1-propanesulfonyl chloride (81 μL, 0.72 mmol), and the reaction mixture was stirred at room temperature overnight. Water was added, the mixture extracted with CH_2Cl_2 (3 × 20 mL), dried (Na_2SO_4), filtered, and concentrated. Flash chromatography (silica, hexane:EtOAc 1:2) afforded the title compound (220 mg, 56%) as a white solid. ^{1}H NMR (400 MHz, $CDCl_3$) δ 7.82 (br s, 1H), 7.29−7.15 (m, 5H), 7.10−7.03 (m, 2H), 3.23−3.14 (m, 2H), 2.90−2.70 (m, 4H), 2.42 (s, 3H), 2.01−1.88 (m, 2H), 1.75−1.65 (m, 4H), 1.41−1.31 (m, 2H), 1.06 (t, J = 7.5 Hz, 3H). ^{13}C NMR (126 MHz, $CDCl_3$) δ 160.8, 149.0, 142.3, 136.8, 135.3, 135.0, 133.8, 133.4, 130.6, 129.9, 129.1, 128.2, 127.4, 123.1, 57.2, 52.9, 25.4, 23.3, 17.5, 13.0, 10.9. HRMS Calcd for $[C_{25}H_{28}Cl_2N_4O_4S + H]$: 551.1287. Found: 551.1313. HPLC: 100%.

*4-(2-(2,4-Dichlorophenyl)-5-methyl-4-(piperidin-1-ylcarbamoyl)-1H-imidazol-1-yl)phenyl-3-fluoropropane-1-sulfonate (**11c**).* A suspension of compound **10** (200 mg, 0.45 mmol) in dry CH_2Cl_2 (3 mL) was treated with Et_3N (45 mg, 0.45 mmol) at rt. The resulting mixture was cooled to −78 °C, and 3-fluoropropane-1-sulfonyl chloride (72 mg, 0.45 mmol) in dry CH_2Cl_2 (0.5 mL) was added dropwise. After 1 h 40 min at −78 °C was added 3-fluoropropane-1-sulfonyl chloride (72 mg, 0.45 mmol) and after a total of 4 h 40 min was added Et_3N

DOI: 10.1021/acs.jmedchem.7b00861
J. Med. Chem. 2017, 60, 9545−9564

(55 mg, 0.54 mmol). The reaction was allowed to reach rt overnight. It was then cooled to 0 °C and Et_3N (55 mg, 0.54 mmol) was added, followed by 3-fluoropropane-1-sulfonyl chloride (72 mg, 0.45 mmol) after a total of 19 h. After 1 h, the reaction mixture was washed with water and concentrated in vacuo. The product was purified by HPLC (30−100% CH_3CN in aqueous NH_4OAc (0.1 M) over 40 min) to yield the title compound as a white solid (160 mg, 63%). ^1H NMR (400 MHz, $CDCl_3$) δ 7.88 (br s, 1H), 7.39−7.17 (m, 5H), 7.11 (d, J = 8.8 Hz, 2H), 4.58 (dt, J = 5.5, 46.8 Hz, 2H), 3.53−3.33 (m, 2H), 2.92−2.71 (m, 4H), 2.45 (s, 3H), 2.40−2.23 (m, 2H), 1.83−1.62 (m, 4H), 1.46−1.33 (m, 2H). HRMS Calcd for $[C_{25}H_{27}Cl_2FN_4O_4S + H]$: 569.119. Found: 569.1192. HPLC: 100%.

*4-(2-(2,4-Dichlorophenyl)-5-methyl-4-(piperidin-1-ylcarbamoyl)-1H-imidazol-1-yl)phenyl 3,3,3-trifluoropropane-1-sulfonate Methanesulfonic Acid Salt (**11d**).* A solution of compound **10** (0.89 g, 2.00 mmol) in CH_2Cl_2 (20 mL) was cooled to 0 °C then treated with Et_3N (0.35 mL, 2.4 mmol), followed by 3,3,3-trifluoropropanesulfonyl chloride (prepared by an analogous method to that described in WO00/010968 for the butyl homologue) (0.35 mL, 2.40 mmol). The reaction mixture was stirred at rt overnight. TLC showed remaining starting material, and so another portion of Et_3N and 3,3,3-trifluoropropanesulfonyl chloride was added and the reaction mixture stirred for additional 2 h. Water was added, and the product was extracted with CH_2Cl_2, dried (Na_2SO_4), filtered, and concentrated in vacuo. Flash chromatography (33−100% EtOAc in hexane) followed by recrystallization (hexane:EtOAc) afforded the title compound (700 mg, 59%) as a colorless solid. ^1H NMR (400 MHz, $CDCl_3$) δ 7.92 (s, 1H), 7.34−7.24 (m, 5H), 7.20−7.13 (m, 2H), 3.54−3.48 (m, 2H), 3.00−2.82 (m, 4H), 2.84−2.73 (m, 2H), 2.50 (s, 3 H), 1.83−1.72 (m, 4 H), 1.49−1.39 (m, 2H). HRMS Calcd for $[C_{26}H_{29}Cl_2F_3N_4O_7S_2 + H]$: 605.1004. Found: 605.1012. HPLC: 100%.

*4-(2-(2,4-Dichlorophenyl)-5-methyl-4-(piperidin-1-ylcarbamoyl)-1H-imidazol-1-yl)phenyl butane-1-sulfonate (**11e**).* A solution of compound **10** (320 mg, 0.72 mmol) in CH_2Cl_2 (10 mL) was cooled to 0 °C. Et_3N (100 μL, 0.72 mmol) was added followed by 1-butanesulfonyl chloride (93 μL, 0.72 mmol), and the reaction mixture was stirred at rt overnight. Water was added, and the mixture extracted with CH_2Cl_2 (3 × 20 mL), dried (Na_2SO_4), filtered, and concentrated in vacuo. Flash chromatography (silica, hexane:EtOAc 1:2) afforded the title compound (230 mg, 57%) as a white solid. ^1H NMR (400 MHz, $CDCl_3$) δ 7.82 (br s, 1H), 7.27−7.16 (m, 5H), 7.09−7.04 (m, 2H), 3.23−3.17 (m, 2H), 2.92−2.68 (m, 4H), 2.42 (s, 3H), 1.93−1.84 (m, 2H), 1.74−1.66 (m, 4H), 1.50−1.40 (m, 2H), 1.40−1.33 (m, 2H), 0.91 (t, J = 7.4 Hz, 3H). MS m/z 588 (M + Na). HRMS Calcd for $[C_{26}H_{30}Cl_2N_4O_4S + H]$: 565.1443. Found: 565.1450. HPLC: 100%.

*4-(2-(2,4-Dichlorophenyl)-5-methyl-4-(piperidin-1-ylcarbamoyl)-1H-imidazol-1-yl)-phenyl-4,4,4-trifluorobutane-1-sulfonate (**11f**).* A solution of compound **10** (0.49 g, 1.20 mmol) in CH_2Cl_2 (20 mL) was cooled to 0 °C and treated with Et_3N (0.67 mL, 4.8 mmol), followed by 4,4,4-trifluorobutane-1-sulfonyl chloride (prepared as described in WO00/010968) (0.38 g, 1.80 mmol). The reaction mixture was stirred at rt for 3 h. TLC showed remaining starting material, so another portion of Et_3N and 4,4,4-trifluorobutane-1-sulfonyl chloride was added and the reaction mixture stirred overnight. Water was added, then the mixture was extracted with CH_2Cl_2. The organic extracts were dried (Na_2SO_4), filtered, and concentrated in vacuo. Flash chromatography (33−100% EtOAc in hexane) followed by recrystallization (hexane:EtOAc) afforded the title compound (0.45 g, 61%) as a colorless solid. ^1H NMR (400 MHz, $CDCl_3$) δ 7.92 (br s, 1H), 7.34−7.22 (m, 5H), 7.15 (d, J = 8.7 Hz, 2H), 3.38 (t, J = 7.3 Hz, 2H), 3.12−2.74 (m, 4H), 2.49 (s, 3H), 2.43−2.32 (m, 2H), 2.32−2.22 (m, 2H), 1.82−1.74 (m, 4H), 1.50−1.40 (m, 2H). HRMS Calcd for $[C_{26}H_{27}Cl_2F_3N_4O_4S + H]$: 619.1160. Found: 619.1148. HPLC: 96.9%.

*4-(2-(2,4-Dichlorophenyl)-5-methyl-4-(piperidin-1-ylcarbamoyl)-1H-imidazol-1-yl)phenyl 3-methylbutane-1-sulfonate (**11g**).* A solution of compound **10** (50 mg, 0.11 mmol) in CH_2Cl_2 (3 mL) was cooled to 0 °C then treated with Et_3N (20 μL, 0.13 mmol). The resulting mixture was cooled to −78 °C, then 3-methylbutane-1-sulfonyl chloride (23 mg, 0.13 mmol) carefully added. The reaction was stirred at −78 °C for 1.5 h. Water was added, then the mixture was extracted with CH_2Cl_2. The organic extracts were dried, filtered, and concentrated in vacuo to give a residue which was purified by HPLC to deliver the title compound (46 mg, 71%) as a solid. ^1H NMR (400 MHz, $CDCl_3$) δ 7.86 (s, 1H), 7.31−7.20 (m, 5H), 7.14−7.08 (m, 2H), 3.27−3.20 (m, 2H), 2.89−2.76 (m, 4H), 2.46 (s, 3H), 1.87−1.79 (m, 2H), 1.78−1.68 (m, 5H), 1.44−1.36 (m, 2H), 0.93 (d, J = 6.5 Hz, 6H). HRMS Calcd for $[C_{26}H_{27}Cl_2F_3N_4O_4S + H]$: 579.1600. Found: 579.1584. HPLC: 100%.

*4-(2-(2,4-Dichlorophenyl)-5-methyl-4-(piperidin-1-ylcarbamoyl)-1H-imidazol-1-yl)phenyl-3,3-dimethylbutane-1-sulfonate (**11h**).* A solution of compound **10** (50 mg, 0.11 mmol) in CH_2Cl_2 (3 mL) was cooled to 0 °C and treated with Et_3N (20 μL, 0.13 mmol). The resulting mixture was cooled to −78 °C, and 3,3-dimethylbutane-1-sulfonyl chloride (25 mg, 0.13 mmol) was carefully added. The reaction was stirred at −78 °C for 2 h. Water was added, then the mixture extracted with CH_2Cl_2. The organic extracts were dried, filtered, and concentrated in vacuo to give a residue which was purified by preparative HPLC to deliver the title compound (46 mg, 69%) as a solid. ^1H NMR (400 MHz, $CDCl_3$) δ 7.85 (s, 1H), 7.32−7.17 (m, 5H), 7.11−7.09 (d, J = 8.7 Hz, 2H), 3.26−3.15 (m, 2H), 2.92−2.74 (m, 4H), 2.46 (s, 3H), 1.87−1.78 (m, 2H), 1.77−1.68 (m, 5H), 1.46−1.34 (m, 2H), 0.92 (s, 9H). HRMS Calcd for $[C_{28}H_{34}Cl_2N_4O_4S + H]$: 593.1756. Found: 593.1755. HPLC: 100%.

*Racemic 1-(4-(Benzyloxy)phenyl)-2-(2,4-dichlorophenyl)-N-(3-hydroxypiperidin-1-yl)-5-methyl-1H-imidazole-4-carboxamide (**12a**).* Compound **4** (752 mg, 1.66 mmol) and $SOCl_2$ (33.2 mmol) were mixed, and the resulting mixture was refluxed for 1.5 h. Excess $SOCl_2$ was removed under reduced pressure and the residue was azeotroped with toluene. 3-Hydroxy-1-aminopiperidine (6.64 mmol) was mixed with CH_2Cl_2 (15 mL) and THF (2 mL) and Et_3N (13.28 mmol). The mixture was cooled to −20 °C under a nitrogen atmosphere. A THF (5 mL) mixture of the acid chloride from above was added dropwise during 20 min. The resulting mixture was allowed to slowly warm to rt and stirred overnight. Aqueous NaOH (1 M, 5 mL) and EtOH (15 mL) were added, and the mixture was heated to 40 °C for 15 min. The reaction mixture was then diluted to 50 mL with CH_2Cl_2 and washed with water (2 × 20 mL) and brine (20 mL). The organic layer was dried ($MgSO_4$), filtered, and concentrated in vacuo. The residue was purified by flash chromatography (8% EtOH in CH_2Cl_2) and then by reverse phase HPLC (Kromasil C8, 60% CH_3CN in aqueous NH_4OAc (0.1 M)). The product fraction was concentrated in vacuo and then dissolved in CH_2Cl_2 and washed with water several times and then brine. The organic layer was dried ($MgSO_4$), filtered, and concentrated in vacuo to give the title compound (160 mg, 17% yield). ^1H NMR (400 MHz, $CDCl_3$) δ 7.99 (s, 1H), 7.33−7.19 (m, 6H), 7.18−7.07 (m, 2H), 6.90 (d, J = 8.8 Hz, 2H), 6.81 (d, J = 8.8 Hz, 2H), 5.18 (s, 1H), 4.92 (s, 2H), 3.94−3.85 (m, 1H), 3.06−2.97 (m, 1H), 2.85−2.66 (m, 3H), 2.34 (s, 3H), 1.87−1.77 (m, 1H), 1.63−1.50 (m, 2H), 1.46−1.34 (m, 1H); MS m/z 551 (M + H).

*Racemic 1-(4-(Benzyloxy)phenyl)-2-(2,4-dichlorophenyl)-N-(3-hydroxycyclohexyl)-5-methyl-1H-imidazole-4-carboxamide (**12b**).* A suspension of compound **4** (2.00 g, 4.41 mmol) in CH_2Cl_2 (50 mL) was treated with oxalyl chloride (2.80 g, 22.1 mmol) at rt, followed by one drop of DMF. The mixture was stirred at rt for 15 min, after which the solvent was removed in vacuo. The acid chloride was suspended in CH_2Cl_2 (10 mL) and added dropwise to a mixture of 3-aminocyclohexanol (610 mg, 5.29 mmol), aqueous NaOH (1 M, 30 mL), and CH_2Cl_2 (30 mL). After stirring at rt for 2 h, adding more 3-aminocyclohexanol after 1 h 25 min (67 mg, 0.58 mmol) and 1 h 45 min (58 mg, 0.50 mmol), water, and CH_2Cl_2 were added and the phases separated. The organic phase was washed with aqueous HCl (10%) and brine, then dried ($MgSO_4$), filtered, and concentrated in vacuo to yield the crude title compound (2.79 g). ^1H NMR (400 MHz, $CDCl_3$) δ 7.40−7.16 (m, 8H), 7.03−6.88 (m, 4H), 5.01 (s, 2H), 4.44−4.32 (m, 0.5H), 4.18−4.11 (m, 0.5 H), 4.06−3.94 (m, 0.5 H), 3.76−3.66 (m, 0.5 H), 2.46 (s, 3H), 2.03−1.10 (m, 8H). MS m/z 550 (M+H).

*Racemic 1-(4-(Benzyloxy)phenyl)-2-(2,4-dichlorophenyl)-N-((trans)-2-hydroxycyclohexyl)-5-methyl-1H-imidazole-4-carboxamide (**12c**).* A suspension of compound **4** (2.00 g, 4.41 mmol) in CH_2Cl_2 (100 mL) was treated with oxalyl chloride (2.80 g, 22.1 mmol) at rt, followed by one drop of DMF. The mixture was stirred at rt for

DOI: 10.1021/acs.jmedchem.7b00861
J. Med. Chem. 2017, 60, 9545−9564

35 min, after which the mixture was concentrated in vacuo. The acid chloride was suspended in CH_2Cl_2 (10 mL) and added dropwise to a mixture of *trans*-2-aminocyclohexanol hydrochloride (802 mg, 5.29 mmol), aqueous NaOH (1 M, 30 mL), and CH_2Cl_2 (30 mL). After stirring at rt for 2 h, water/CH_2Cl_2 were added, and the phases were separated. The organic phase was washed with aqueous HCl (10%) and brine, dried ($MgSO_4$), filtered, and concentrated in vacuo to yield the crude title compound (2.69 g). ^{1}H NMR (400 MHz, $CDCl_3$) δ 7.94 (s, 1H), 7.37−7.25 (m, 6H), 7.23−7.17 (m, 2H), 6.97 (d, J = 8.6 Hz, 2H), 6.89 (d, J = 8.6 Hz, 2H), 5.23 (s, 1H), 4.98 (s, 2H), 3.80−3.62 (m, 1H), 3.59−3.42 (m, 1H), 2.42 (s, 3H), 2.14−1.93 (m, 2H), 1.75−1.59 (m, 2H), 1.39−1.14 (m, 4H). MS m/z 550 (M + H).

*Racemic 1-(4-(Benzyloxy)phenyl)-2-(2,4-dichlorophenyl)-N-((cis)-2-hydroxycyclohexyl)-5-methyl-1H-imidazole-4-carboxamide (**12d**).* A suspension of compound **4** (2.00 g, 4.41 mmol) in CH_2Cl_2 (100 mL) was treated with oxalyl chloride (2.85 g, 22.5 mmol) at rt, followed by one drop of DMF. The mixture was stirred at rt for 20 min, after which the solvents were evaporated under reduced pressure. The acid chloride was suspended in CH_2Cl_2 (10 mL) and added dropwise to a mixture of *cis*-2-aminocyclohexanol hydrochloride (816 mg, 5.38 mmol), aqueous NaOH (1M, 30 mL) and CH_2Cl_2 (30 mL). After stirring at rt for 2 h, water was added and the phases were separated. The organic phase was washed with aqueous HCl (0.1 M) and brine, dried ($MgSO_4$), filtered, and concentrated in vacuo to yield the title compound (2.40 g, 99%). ^{1}HNMR (400 MHz, $CDCl_3$) δ 7.45 (d, J = 7.8 Hz, 1H), 7.41−7.16 (m, 8H), 6.98 (d, J = 8.8 Hz, 2H), 6.90 (d, J = 8.8 Hz, 2H), 5.01 (s, 2H), 4.16−4.08 (m, 1H), 4.03−3.96 (m, 1H), 2.89 (br s, 1H), 2.43 (s, 3H), 1.83−1.54 (m, 6H), 1.47−1.32 (m, 2H). MS m/z 550 (M + H).

*1-(4-(Benzyloxy)phenyl)-2-(2,4-dichlorophenyl)-5-methyl-N-(4-(trifluoromethoxy)phenyl)-1H-imidazole-4-carboxamide (**12e**).* A suspension of compound **4** (1.00 g, 2.21 mmol) in CH_2Cl_2 (15 mL) was treated with oxalyl chloride (1.40 g, 11.0 mmol) at rt, followed by one drop of DMF. The mixture was stirred at rt for 15 min, after which the solvents were evaporated under reduced pressure. A mixture of 4-trifluoromethoxy-phenylamine (469 mg, 2.65 mmol), Et_3N (313 mg, 3.09 mmol), and CH_2Cl_2 (5 mL) was added dropwise to the acid chloride suspended in CH_2Cl_2 (15 mL). The reaction mixture was stirred at rt for 2 h and 10 min. CH_2Cl_2 was added, and the resulting mixture was washed with aqueous HCl (10%) and brine, dried ($MgSO_4$), filtered, and evaporated to yield the crude title compound (1.42 g). ^{1}H NMR (400 MHz, $CDCl_3$) δ 9.37 (br s, 1H), 7.76−7.74 (m, 2H), 7.39−7.16 (m, 10H), 7.05−6.93 (m, 4H), 5.03 (s, 2H), 2.50 (s, 3H). MS m/z 612 (M + H).

*1-(4-(Benzyloxy)phenyl)-2-(2,4-dichlorophenyl)-N-(6-fluoropyridin-3-yl)-5-methyl-1H-imidazole-4-carboxamide (**12f**).* A suspension of compound **4** (1.00 g, 2.21 mmol) in CH_2Cl_2 (15 mL) was treated with oxalyl chloride (1.40 g, 11.0 mmol) at rt, followed by one drop of DMF. The mixture was stirred at rt for 5 min after which the solvents were removed in vacuo. The acid chloride was suspended in CH_2Cl_2 (8 mL) then treated dropwise with a mixture of 6-fluoro-pyridin-3-ylamine (297 mg, 2.65 mmol), Et_3N (313 mg, 3.09 mmol), and CH_2Cl_2 (7 mL). Stirring was continued at rt for 75 min, after which CH_2Cl_2 was added and the resulting mixture washed with aqueous HCl (10%) and brine. The organic extracts were dried ($MgSO_4$), filtered, and concentrated in vacuo to yield the crude title compound (1.19 g). ^{1}H NMR (400 MHz, $CDCl_3$) δ 9.24 (s, 1H), 8.39−8.33 (m, 2H), 7.39−6.89 (m, 3H), 5.02 (s, 2H), 2.49 (s, 3H). MS m/z 547 (M + H).

*1-(4-(Benzyloxy)phenyl)-2-(2,4-dichlorophenyl)-5-methyl-N-(6-(trifluoromethyl)pyridin-3-yl)-1H-imidazole-4-carboxamide (**12g**).* A suspension of compound **4** (1.00 g, 2.21 mmol) in CH_2Cl_2 (15 mL) was treated with oxalyl chloride (1.40 g, 11.03 mmol) at rt, followed by one drop of DMF. The mixture was stirred at rt for 5 min, after which the solvents were removed in vacuo. The acid chloride was suspended in CH_2Cl_2 (8 mL) then treated dropwise with a solution of 6-trifluoromethyl-pyridin-3-ylamine (407 mg, 2.51 mmol) and Et_3N (360 mg, 3.56 mmol) in CH_2Cl_2 (7 mL). The reaction mixture was stirred at rt for 1.5 h then diluted with CH_2Cl_2 and washed with aqueous HCl (10% w/w) and brine. The organic extracts were dried ($MgSO_4$), filtered, and concentrated in vacuo to yield the crude title product (1.32 g). ^{1}H NMR (400 MHz, $CDCl_3$) δ 9.50 (s, 1H), 8.82 (d, J = 2.0 Hz, 1H), 8.55 (dd, J = 2.0, 8.6 Hz, 1H), 7.65 (d, J = 8.6 Hz, 1H), 7.40−7.21 (m, 7H), 7.06−6.89 (m, 5H), 5.03 (s, 2H), 2.50 (s, 3H). MS m/z 597 (M + H).

*1-(4-(Benzyloxy)phenyl)-2-(2,4-dichlorophenyl)-5-methyl-N-(5-methylpyridin-2-yl)-1H-imidazole-4-carboxamide (**12h**).* A suspension of compound **4** (3.00 g, 6.62 mmol) in CH_2Cl_2 (70 mL) was treated with oxalyl chloride (4.20 g, 33.1 mmol) at rt, followed by one drop of DMF. The mixture was stirred at rt for 5 min, after which the solvents were evaporated under reduced pressure. A mixture of 5-methyl-pyridin-2-ylamine (816 mg, 7.54 mmol), Et_3N (890 mg, 8.80 mmol), and CH_2Cl_2 (20 mL) was added dropwise to the acid chloride suspended in CH_2Cl_2 (20 mL). The reaction mixture was stirred at rt for 30 min. CH_2Cl_2 was added, and the resulting mixture was washed with aqueous HCl (10%) and brine, dried ($MgSO_4$), filtered, and evaporated. The residue was purified by flash chromatography (20−30% EtOAc in heptane) to yield the title compound as a white solid (980 mg, 27%). ^{1}H NMR (400 MHz, pyridine-d_5) δ 10.11 (s, 1H), 8.52 (s, 1H), 8.04 (s, 1H), 7.40−6.88 (m, 3H), 4.80 (s, 2H), 2.39 (s, 3H), 1.88 (s, 3H). MS m/z 543 (M + H).

*Racemic 2-(2,4-Dichlorophenyl)-1-(4-hydroxyphenyl)-N-(3-hydroxypiperidin-1-yl)-5-methyl-1H-imidazole-4-carboxamide (**13a**).* A mixture of racemic 1-(4-(benzyloxy)phenyl)-2-(2,4-dichlorophenyl)-*N*-(3-hydroxypiperidin-1-yl)-5-methyl-1*H*-imidazole-4-carboxamide (160 mg, 0.29 mmol) and dimethyl sulfide (1.45 mmol) in CH_2Cl_2 under nitrogen atmosphere were treated dropwise with $BF_3{\cdot}OEt_2$ (1.45 mmol). The resulting mixture was stirred for 4 days at ambient temperature while continuously adding small volumes of CH_2Cl_2 and 1,4-dioxane. EtOH was added, and the mixture was stirred for 30 min and then concentrated in vacuo. The residue was dissolved in EtOAc (50 mL) and washed with water (2 × 20 mL) and brine (20 mL). Th eorganic layer was dried (Na_2SO_4), filtered, and concentrated in vacuo to give the title compound (127 mg, 95%) as a white solid. MS m/z 461 (M + H).

*Racemic 2-(2,4-Dichlorophenyl)-N-(3-hydroxycyclohexyl)-1-(4-hydroxyphenyl)-5-methyl-1H-imidazole-4-carboxamide (**13b**).* A suspension of crude 1-(4-(benzyloxy)phenyl)-2-(2,4-dichlorophenyl)-*N*-(3-hydroxycyclohexyl)-5-methyl-1*H*-imidazole-4-carboxamide (2.79 g, 5.07 mmol) in CH_2Cl_2 (50 mL), and dimethyl sulfide (3.15 g, 50.7 mmol) was treated with boron trifluoride diethyl etherate (5.77 g, 50.7 mmol). The reaction mixture was stirred at rt for 36 h (dark), adding more dimethyl sulfide (3.15 g, 50.7 mmol) and boron trifluoride (5.77 g, 50.7 mmol) after 16 h. The solvent was evaporated and the residue dissolved in EtOAc/water. The phases were separated and the organic phase dried ($MgSO_4$), filtered, and concentrated in vacuo to yield the crude title compound (2.54 g). MS m/z 460 (M + H).

*Racemic 2-(2,4-Dichlorophenyl)-N-((trans)-2-hydroxycyclohexyl)-1-(4-hydroxyphenyl)-5-methyl-1H-imidazole-4-carboxamide (**13c**).* Crude racemic 1-(4-(benzyloxy)phenyl)-2-(2,4-dichlorophenyl)-*N*-((*trans*)-2-hydroxycyclohexyl)-5-methyl-1*H*-imidazole-4-carboxamide (2.68 g, 4.87 mmol) was suspended in HBr (33% in AcOH, 60 mL). The mixture was stirred at rt, in the dark, for 1 h 20 min. EtOH was added and the mixture concentrated in vacuo. The residue was dissolved in MeOH and neutralized with $NaHCO_3$ (1 M, aq). One spoon of K_2CO_3 was added, and the mixture was stirred at rt for 1 h. The solvent was evaporated, and the resulting mixture extracted with toluene followed by THF. The combined organic phases were washed with aqueous HCl (10%) and brine, dried ($MgSO_4$), filtered, and evaporated. The product was purified by HPLC (30−100% CH_3CN in aqueous NH_4OAc (0.1 M) over 40 min) to yield the title compound as a white solid (829 mg, yield over 2 steps 41%). ^{1}H NMR (400 MHz, $CDCl_3$) δ 7.36−7.18 (m, 4H), 6.86−6.66 (m, 4H), 5.28 (s, 1H), 4.60 (br s, 1H), 3.85−3.74 (m, 1H), 3.52−3.41 (m, 1H), 2.37 (s, 3H), 2.13−1.97 (m, 2H), 1.78−1.67 (m, 2H), 1.44−1.15 (m, 4H). MS m/z 460 (M + H).

*Racemic 2-(2,4-Dichlorophenyl)-N-((cis)-2-hydroxycyclohexyl)-1-(4-hydroxyphenyl)-5-methyl-1H-imidazole-4-carboxamide (**13d**).* A suspension of racemic 1-(4-(benzyloxy)phenyl)-2-(2,4-dichlorophenyl)-*N*-((*cis*)-2-hydroxycyclohexyl)-5-methyl-1*H*-imidazole-4-carboxamide (2.38 g, 4.33 mmol) in HBr (33% in AcOH, 50 mL). The reaction mixture was stirred at rt, in the dark, for 1 h. EtOH was added and the solvents were evaporated under reduced pressure. The residue was dissolved in MeOH and neutralized with aqueous $NaHCO_3$ (1 M).

DOI: 10.1021/acs.jmedchem.7b00861
J. Med. Chem. 2017, 60, 9545−9564

The solvent was evaporated and the mixture dissolved in water/CH_2Cl_2. The phases were separated, and the organic phase was washed with brine, dried ($MgSO_4$), filtered, and evaporated. The residue was dissolved in MeOH and one spoon of K_2CO_3 was added, and the resulting mixture was stirred at rt for 1 h before the solvent was evaporated. The residue was resuspended in CH_2Cl_2 and washed with aqueous HCl (10%), and the solvents were evaporated. The residue was dissolved in THF, dried ($MgSO_4$), filtered, and evaporated to yield the crude title compound (2.10 g). ^{1}H NMR (400 MHz, THF-d_8) δ 8.65 (d, J = 7.3 Hz, 1H), 7.66 (d, J = 8.3 Hz, 1H), 7.55 (d, J = 1.7 Hz, 1H), 7.25 (dd, J = 1.7, 8.3, 1H), 7.18 (d, J = 8.6 Hz, 2H), 6.79 (d, J = 8.6 Hz, 2H), 3.99−3.91 (m, 1H), 3.91−3.82 (m, 1H), 3.64−3.55 (m, 1H), 2.47 (s, 3H), 1.86−1.63 (m, 5H), 1.58−1.44 (m, 1H), 1.38−1.28 (m, 2H). MS m/z 460 (M + H).

*2-(2,4-Dichlorophenyl)-1-(4-hydroxyphenyl)-5-methyl-N-(4-(trifluoromethoxy)pheny1)-1H-imidazole-4-carboxamide (**13e**).* Crude **12e** (1.35 g, 2.20 mmol) was suspended in HBr (33% in AcOH, 25 mL). The reaction mixture was stirred at rt, in the dark, for 1 h. EtOH was added, and the solvents were evaporated at reduced pressure. The residue was dissolved in MeOH and neutralized with aqueous $NaHCO_3$ (1 M). The solvent was evaporated and the mixture dissolved in water/CH_2Cl_2. The phases were separated and the organic phase was washed with brine, dried ($MgSO_4$), filtered, and concentrated in vacuo to yield the crude title compound (1.10 g). ^{1}H NMR (400 MHz, $CDCl_3$) δ 7.73−7.71 (m, 2H), 7.39−7.16 (m, 5H), 6.94−6.76 (m, 4H), 2.45 (s, 3H). MS m/z 522 (M + H).

*2-(2,4-Dichlorophenyl)-N-(6-fluoropyridin-3-yl)-1-(4-hydroxyphenyl)-5-methyl-1H-imidazole-4-carboxamide (**13f**).* Compound **12f** (1.15 g, 2.10 mmol) was suspended in HBr (33% in AcOH, 25 mL). The reaction mixture was stirred at rt, in the dark, for 2 h 30 min. EtOH was added, and the solvents were evaporated under reduced pressure. The residue was dissolved in MeOH and neutralized with aqueous $NaHCO_3$ (1 M). The solvent was evaporated and the mixture dissolved in water/CH_2Cl_2. The phases were separated, and the organic phase was washed with brine, dried ($MgSO_4$), filtered, and concentrated in vacuo to give a residue which was purified by HPLC (30−60% CH_3CN in NH_4OAc (0.1 M) over 40 min, then 100% CH_3CN) to yield the title compound as a white solid (519 mg, yield over 2 steps 53%). ^{1}H NMR (400 MHz, $CDCl_3$) δ 9.14 (s, 1H), 8.37−8.30 (m, 2H), 7.34 (s, 1H), 7.25−7.20 (m, 2H), 6.96−6.90 (m, 3H), 6.79−6.77 (m, 2H), 2.48 (s, 3H). MS m/z 457 (M + H).

*2-(2,4-Dichlorophenyl)-1-(4-hydroxyphenyl)-5-methyl-N-(6-(trifluoromethyl)pyridin-3-yl)-1H-imidazole-4-carboxamide (**13g**).* A suspension of crude **12g** (1.17 g, 1.96 mmol) in CH_2Cl_2 (6 mL) and dimethyl sulfide (1.22 g, 19.6 mmol) was treated with boron trifluoride (2.78 g, 19.6 mmol). The reaction mixture was stirred at rt for 31 h (dark). Water and CH_2Cl_2 were added and the phases separated. The organic phase was washed with water (×4) and concentrated in vacuo. The residue was dissolved in MeOH and stirred at rt for 20 h before water was added and the MeOH removed in vacuo. The resulting mixture was extracted with Et_2O (×2), and the combined organic phases were washed with brine, dried ($MgSO_4$), filtered, and concentrated in vacuo to yield the crude title compound (776 mg). ^{1}H NMR (400 MHz, $CDCl_3$) δ 9.29 (s, 1H), 8.75 (d, J = 2.1 Hz, 1H), 8.54 (dd, J = 2.1, 8.6 Hz, 1H), 7.64 (d, J = 8.6 Hz, 1H), 7.33 (d, J = 1.7 Hz, 1H), 7.27−7.19 (m, 2H), 6.96 (d, J = 8.7 Hz, 2H), 6.78 (d, J = 8.7 Hz, 1H), 5.51 (br s, 1H), 2.48 (s, 3H). MS m/z 507 (M + H).

*2-(2,4-Dichlorophenyl)-1-(4-hydroxyphenyl)-5-methyl-N-(5-methylpyridin-2-yl)-1H-imidazole-4-carboxamide (**13h**).* Compound **12h** (958 mg, 1.76 mmol) was suspended in HBr (33% in AcOH, 25 mL). The reaction mixture was stirred at rt, in the dark, for 1 h. EtOH was added, and the solvents were evaporated under reduced pressure. The residue was dissolved in MeOH and neutralized with aqueous $NaHCO_3$ (1 M). The solvent was evaporated and the mixture dissolved in water/CH_2Cl_2. The phases were separated, and the organic phase was washed with brine, dried ($MgSO_4$), filtered, and evaporated to yield the title compound (772 mg, 97%). ^{1}H NMR (400 MHz, pyridine-d_5) δ 10.12 (s, 1H), 8.52 (s, 1H), 8.03 (s, 1H), 7.40−6.89 (m, 8H), 2.42 (s, 3H), 1.88 (s, 3H). MS m/z 453 (M + H).

*Racemic 4-(2-(2,4-Dichlorophenyl)-4-(3-hydroxypiperidin-1-ylcarbamoyl)-5-methyl-1H-imidazol-1-yl)phenyl 3,3,3-trifluoropropane-1-sulfonate (**14a**).* A solution of 2-(2,4-dichlorophenyl)-1-(4-hydroxyphenyl)-*N*-(3-hydroxypiperidin-1-yl)-5-methyl-1*H*-imidazole-4-carboxamide (118 mg, 0.25 mmol) in CH_2Cl_2 (1 mL), and THF (1 mL) was treated with Et_3N (0.25 mmol) under a nitrogen atmosphere. The solution was cooled to −78 °C, and a solution of 3,3,3-trifluoropropane-1-sulfonyl chloride in CH_2Cl_2 (1 mL) was added slowly while monitoring the progress with LC-MS. The reaction mixture was quenched by addition of EtOH. The reaction mixture was concentrated in vacuo, and the residue was purified by reverse phase HPLC (Kromasil C8, 5−100% CH_3CN in aqueous NH_4OAc (0.1 M)) and by flash chromatography (8% EtOH in CH_2Cl_2). The product was freeze-dried to give the title compound (40 mg, 25%) as a white powder. ^{1}H NMR (CD_3OD) δ 7.52−7.44 (m, 2H), 7.44−7.34 (m, 5H), 3.91−3.82 (m, 1H), 3.77−3.69 (m, 2H), 3.11 (dd, J = 3.0, 10.1 Hz, 1H), 2.95−2.80 (m, 3H), 2.74−2.58 (m, 2H), 2.46 (s, 3H), 1.95−1.75 (m, 2H), 1.73−1.62 (m, 1H), 1.44−1.31 (m, 1H). MS m/z 621 (M + H). HRMS Calcd for $[C_{25}H_{25}Cl_2F_3N_4O_5S$ + H]: 621.0954. Found: 621.0919. HPLC: 100%.

*Racemic 4-(2-(2,4-Dichlorophenyl)-4-((trans)-3-hydroxycyclohexylcarbamoyl)-5-methyl-1H-imidazol-1-yl)phenyl 3,3,3-trifluoropropane-1-sulfonate (**14b**).* A suspension of crude 2-(2,4-dichlorophenyl)-*N*-(3-hydroxycyclohexyl)-1-(4-hydroxyphenyl)-5-methyl-1*H*-imidazole-4-carboxamide (2.53 mg, 5.49 mmol) in dry CH_2Cl_2 (20 mL) was treated with Et_3N (667 mg, 6.59 mmol) at rt. The resulting mixture was cooled to −78 °C, and 3,3,3-trifluoropropane-1-sulfonyl chloride (1.30 mg, 6.59 mmol) was added dropwise. After stirring at −78 °C for 2 h 45 min, the reaction mixture was allowed to reach rt, upon which it was washed with water and evaporated. The stereoisomers were separated by HPLC (30−100% CH_3CN in aqueous NH_4OAc (0.1 M)) to yield the *trans*-hydroxycyclohexyl product (205 mg, 7.5% over 3 steps) as a white solid. ^{1}H NMR (400 MHz, $CDCl_3$) δ 7.34−7.23 (m, 5H), 7.20−7.10 (m, 3H), 4.45−4.33 (m, 1H), 4.17−4.10 (m, 1H), 3.55−3.47 (m, 2H), 2.87−2.73 (m, 2H), 2.49 (s, 3H), 2.05−1.51 (m, 8H), 1.48−1.36 (m, 1H). HRMS Calcd for $[C_{26}H_{26}Cl_2F_3N_3O_5S$ + H]: 620.1001. Found: 620.1028. HPLC: 100%.

*(−) 4-(2-(2,4-Dichlorophenyl)-4-((trans)-2-hydroxycyclohexylcarbamoyl)-5-methyl-1H-imidazol-1-yl)phenyl 3,3,3-trifluoropropane-1-sulfonate (**14c**).* A suspension of racemic 2-(2,4-dichlorophenyl)-*N*-((*trans*)-2-hydroxycyclohexyl)-1-(4-hydroxyphenyl)-5-methyl-1*H*-imidazole-4-carboxamide (829 mg, 1.80 mmol) in dry CH_2Cl_2 (10 mL) was treated with Et_3N (182 mg, 1.80 mmol) at rt. The resulting mixture was cooled to −78 °C and 3,3,3-trifluoropropane-1-sulfonyl chloride (354 mg, 1.80 mmol) dry CH_2Cl_2 (1 mL) was added dropwise. After stirring at −78 °C for 1 h, the reaction mixture was washed with water and evaporated. The racemic product was purified by HPLC (30−100% CH_3CN in aqueous NH_4OAc (0.1 M) over 40 min) to yield the title compound as a white solid (710 mg, 64%). ^{1}H NMR (400 MHz, $CDCl_3$) δ 7.29−7.06 (m, 8H), 3.82−3.62 (m, 2H), 3.50−3.41 (m, 2H), 3.41−3.31 (m, 1H), 2.81−2.65 (m, 2H), 2.43 (s, 3H), 2.09−1.90 (m, 2H), 1.75−1.61 (m, 2H), 1.34−1.12 (m, 4H). HRMS Calcd for $[C_{26}H_{26}Cl_2F_3N_3O_5S$ + H): 620.1001. Found: 620.1011. The (−)-enantiomer was separated from the racemate (535 mg, 0.86 mmol) by chiral chromatography (Chiralpak AD, heptane:iPrOH 85:15) to afford the title compound (220 mg) (95.6% ee) as white solid after freeze-drying. $[\alpha]_D$ = −2.9 (c 1.04, CH_3CN). ^{1}H NMR (400 MHz, $CDCl_3$) δ 7.29−7.06 (m, 8H), 3.82−3.62 (m, 2H), 3.50−3.41 (m, 2H), 3.41−3.31 (m, 1H), 2.81−2.65 (m, 2H), 2.43 (s, 3H), 2.09−1.90 (m, 2H), 1.75−1.61 (m, 2H), 1.34−1.12 (m, 4H). HRMS Calcd for $[C_{26}H_{26}Cl_2F_3N_3O_5S$ + H]: 620.1001. Found: 620.0956. HPLC: 100%. Vibrational circular dichroism experiments were unable to unambiguously assign the absolute stereochemistry of the (+) and (−) enantiomers.

*(+)-4-[2-(2,4-Dichlorophenyl)-4-({[cis-2-hydroxycyclohexyl]-amino}carbonyl)-5-methyl-1H-imidazol-1-yl]phenyl-3,3,3-trifluoropropane-1-sulfonate (**14d**).* A suspension of crude racemic 2-(2,4-dichlorophenyl)-*N*-((*cis*)-2-hydroxycyclohexyl)-1-(4-hydroxyphenyl)-5-methyl-1*H*-imidazole-4-carboxamide (2.00 g, 4.34 mmol) in dry CH_2Cl_2 (30 mL) was treated with Et_3N (440 mg, 4.34 mmol) at rt. The resulting mixture was cooled to −78 °C, and 3,3,3-trifluoropropane-1-sulfonyl chloride (854 mg, 4.34 mmol) was added dropwise. After stirring at

DOI: 10.1021/acs.jmedchem.7b00861
J. Med. Chem. 2017, 60, 9545−9564

−78 °C for 2 h 20 min, more Et_3N (2(73 mg, 0.72 mmol)) and 3,3,3-trifluoropropane-1-sulfonyl chloride (2(110 mg, 0.56 mmol)) were added (second addition after 1 h). After 2 h, the reaction mixture was washed with water and evaporated. The racemic product was purified by HPLC (30−100% CH_3CN in aqueous NH_4OAc (0.1 M) over 40 min) to yield the title compounds as a white solid (1.31 g, yield over 2 steps 51%). ^1H NMR (400 MHz, $CDCl_3$) δ 7.38 (d, J = 7.7 Hz, 1H), 7.28−7.16 (m, 5H), 7.09 (d, J = 8.7 Hz, 2H), 4.13−4.02 (m, 1H), 4.00−3.89 (m, 1H), 3.49−3.38 (m, 2H), 2.80−2.65 (m, 2H), 2.42 (s, 3H), 1.78−1.47 (m, 6H), 1.44−1.28 (m, 2H). HRMS Calcd for $[C_{26}H_{26}Cl_2F_3N_3O_5S$ + H]: 620.1001. Found: 620.1025. The (+)-enantiomer was separated from the racemate (1.00 g, 1.61 mmol) by chiral chromatography (Chiralpak AD, heptane/iPrOH 80/20) to yield the title compound (444 mg) (>99.9% ee) as a white powder after freeze-drying. $[\alpha]_D$ = +9.9 (c 1.02, CH_3CN). ^1H NMR (400 MHz, $CDCl_3$) δ 7.38 (d, J = 7.7 Hz, 1H), 7.28−7.16 (m, 5H), 7.09 (d, J = 8.7 Hz, 2H), 4.13−4.02 (m, 1H), 4.00−3.89 (m, 1H), 3.49−3.38 (m, 2H), 2.80−2.65 (m, 2H), 2.63−2.53 (m, 1H), 2.42 (s, 3H), 1.78−1.47 (m, 6H), 1.44−1.28 (m, 2H). HRMS Calcd for $[C_{26}H_{26}Cl_2F_3N_3O_5S$ + H] 620.1001. Found: 620.0945. HPLC: 100%. Vibrational circular dichroism experiments were unable to unambiguously assign the absolute stereochemistry of the (+) and (−) enantiomers.

*4-(2-(2,4-Dichlorophenyl)-5-methyl-4-(4-(trifluoromethoxy)-phenylcarbamoyl)-1H-imidazol-1-yl)phenyl 3,3,3-trifluoropropane-1-sulfonate (**14e**).* A suspension of **13e** (150 mg, 0.29 mmol) in dry CH_2Cl_2 (2 mL) was treated with Et_3N (38 mg, 0.37 mmol) at rt. The resulting mixture was cooled to −78 °C and 3,3,3-trifluoropropane-1-sulfonyl chloride (79 mg, 0.40 mmol) in 0.5 mL of dry CH_2Cl_2 was added dropwise. After stirring at −78 °C for 70 min, the reaction mixture was washed with water and evaporated. The product was purified by HPLC (30−100% CH_3CN in aqueous NH_4OAc (0.1 M) over 35 min) to yield the title compound as a white solid (84 mg, yield over 3 steps 43%). ^1H NMR (400 MHz, $CDCl_3$) δ 9.10 (s, 1H), 7.71 (d, J = 9.0 Hz, 2H), 7.36−7.24 (m, 9H), 7.22−7.15 (m, 4H), 3.54−3.47 (m, 2H), 2.86−2.72 (m, 2H), 2.53 (s, 3H). HRMS Calcd for $[C_{27}H_{19}Cl_2F_6N_3O_5S$ + H]: 682.0405. Found: 682.0403. HPLC: 100%.

*4-(2-(2,4-Dichlorophenyl)-4-(6-fluoropyridin-3-ylcarbamoyl)-5-methyl-1H-imidazol-1-yl)phenyl 3,3,3-trifluoropropane-1-sulfonate (**14f**).* A suspension of 2-(2,4-dichlorophenyl)-*N*-(6-fluoropyridin-3-yl)-1-(4-hydroxyphenyl)-5-methyl-1*H*-imidazole-4-carboxamide (150 mg, 0.33 mmol) in dry CH_2Cl_2 (2 mL) was treated with Et_3N (43 mg, 0.43 mmol) at rt. The resulting mixture was cooled to −78 °C, and 3,3,3-trifluoropropane-1-sulfonyl chloride (90 mg, 0.46 mmol) in dry CH_2Cl_2 (0.5 mL) was added dropwise. After stirring at −78 °C for 2 h 30 min, more 3,3,3-trifluoropropane-1-sulfonyl chloride (14 mg, 0.07 mmol) was added and the mixture stirred for another 2 h. The reaction mixture was washed with water and evaporated. The product was purified by HPLC (30−100% CH_3CN in aqueous NH_4OAc (0.1 M) over 35 min) to yield the title compound as a white solid (133 mg, 66%). ^1H NMR (400 MHz, $CDCl_3$) δ 9.09 (s, 1H), 8.40−8.31 (m, 2H), 7.37−7.24 (m, 5H), 7.19 (d, J = 8.8 Hz, 2H), 6.95−6.88 (m, 1H), 3.55−3−46 (m, 2H), 2.86−2.72 (m, 2H), 2.53 (s, 3H). ^{13}C NMR (126 MHz, $CDCl_3$) δ 161.5, 160.7, 158.9, 148.7, 142.6, 138.4 (d, J = 15.1), 137.2, 135.5 (d, J = 38.6), 134.0, 133.3, 133.0 (d, J = 4.5), 132.7 (d, J = 7.5), 130.8, 130.0, 129.4, 127.7, 127.6, 125.1 (q, J = 276.6), 123.2, 109.5 (d, J = 38.8), 44.6 (q, J = 3.3), 29.3 (q, J = 31.9), 11.0. HRMS Calcd for $[C_{25}H_{18}Cl_2F_4N_4O_4S$ + H]: 617.0440. Found: 617.0473. HPLC: 100%.

*4-(2-(2,4-Dichlorophenyl)-5-methyl-4-(6-(trifluoromethyl)pyridin-3-ylcarbamoyl)-1H-imidazol-1-yl)phenyl 3,3,3-trifluoropropane-1-sulfonate (**14g**).* A suspension of crude **13g** (150 mg, 0.30 mmol) in dry CH_2Cl_2 (2 mL) was treated with Et_3N (39 mg, 0.38 mmol) at rt then cooled to −78 °C. To this was added dropwise 3,3,3-trifluoropropane-1-sulfonyl chloride (91 mg, 0.46 mmol) in dry CH_2Cl_2 (0.5 mL). After stirring at −78 °C for 70 min, the mixture was washed with water and concentrated in vacuo to give a residue which was purified by HPLC (30−100% CH_3CN in aqueous NH_4OAc (0.1 M) over 40 min) to yield the title compound as a white solid (131 mg, yield over 3 steps 52%). ^1H NMR (400 MHz, $CDCl_3$) δ 9.29 (s, 1H), 8.77 (d, J = 2.1 Hz, 1H), 8.56 (dd, J = 2.1, 8.6 Hz, 1H), 7.66 (d, J = 8.6 Hz, 1H), 7.37−7.16 (m, 7H), 3.55−3.46 (m, 2H), 2.86−2.72 (m, 2H), 2.53 (s, 3H). HRMS Calcd for $[C_{26}H_{18}Cl_2F_6N_4O_4S$ + H]: 667.0408. Found: 667.0389. HPLC: 100%.

*4-(2-(2,4-Dichlorophenyl)-5-methyl-4-(5-methylpyridin-2-ylcarbamyl)-1H-imidazol-1-yl)phenyl 3,3,3-trifluoropropane-1-sulfonate (**14h**).* A suspension of **13h** (150 mg, 0.33 mmol) in dry CH_2Cl_2 (2 mL) was treated with Et_3N (44 mg, 0.43 mmol) at rt. The resulting mixture was cooled to −78 °C, and 3,3,3-trifluoropropane-1-sulfonyl chloride (94 mg, 0.48 mmol) in dry CH_2Cl_2 (0.5 mL) was added dropwise. After stirring at −78 °C for 80 min, the reaction mixture was washed with water and evaporated. The product was purified by HPLC (30−100% CH_3CN in aqueous NH_4OAc (0.1 M) over 40 min) to yield the title compound as a white solid (132 mg, 65%). ^1H NMR (400 MHz, $CDCl_3$) δ 9.63 (s, 1H), 8.23 (d, J = 8.4 Hz, 1H), 8.11 (d, J = 1.4 Hz, 1H), 7.51 (dd, J = 2.1, 8.4 Hz, 1H), 7.34−7.24 (m, 5H), 7.18 (d, J = 8.9 Hz, 2H), 3.55−3.44 (m, 2H), 2.86−2.71 (m, 2H), 2.53 (s, 3H), 2.28 (s, 3H). HRMS Calcd for $[C_{26}H_{21}Cl_2F_3N_4O_4S$ + H]: 613.0691. Found: 613.0702. HPLC: 100%.

*2,2,2-Trichloroethyl-1-(4-(benzyloxy)phenyl)-2-(2,4-dichlorophenyl)-5-methyl-1H-imidazole-4-carboxylate (**15**).* A solution of compound **4** (10.0 g, 22.1 mmol) in CH_2Cl_2 (210 mL) was treated with oxalyl chloride (18.5 g, 145 mmol), followed by a few drops of DMF. The mixture was stirred at rt for 2 h, after which the solvents were evaporated. The residue was dissolved in CH_2Cl_2 (80 mL) and the mixture was cooled to 0 °C, upon which 2,2,2-trichloroethanol (3.63 g, 24.3 mmol) was added followed by DIPEA (3.42 g, 26.5 mmol). The ice bath was then removed, and the reaction mixture was stirred at rt for 3 h, adding DMAP (279 mg, 2.28 mmol) after 1 h 40 min. The reaction mixture was diluted with CH_2Cl_2, washed with water, dried ($MgSO_4$), filtered, and concentrated in vacuo to yield the crude title compound (14.9 g). ^1H NMR (400 MHz, $CDCl_3$) δ 7.40−7.14 (m, 8H), 7.04−6.98 (m, 2H), 6.94−6.88 (m, 2H), 5.01 (4H, s), 2.45 (s, 3H). MS m/z 583 (M + H).

*2,2,2-Trichloroethyl-2-(2,4-dichlorophenyl)-1-(4-hydroxyphenyl)-5-methyl-1H-imidazole-4-carboxylate (**16**).* Crude **15** (14.77 g) was dissolved in HBr (33% in AcOH, 200 mL). After having stirred at rt for an additional hour, the reaction mixture was cooled to 0 °C and EtOH was added. The mixture was stirred for 10 min before the solvents were evaporated. The residue was dissolved in MeOH and neutralized with aqueous $NaHCO_3$ (1 M). The solvent was evaporated and the mixture dissolved in CH_2Cl_2. The organic phase was washed with brine and water, dried ($MgSO_4$), filtered, and concentrated in vacuo to yield the title compound (10.4 g, 95% over 2 steps). ^1H NMR (400 MHz, $CDCl_3$) δ 8.63 (br s, 1H), 7.25−7.08 (m, 3H), 6.86−6.68 (m, 4H), 4.95 (s, 2H), 2.43 (s, 3H). MS m/z 493 (M + H).

*2,2,2-Trichloroethyl-2-(2,4-dichlorophenyl)-5-methyl-1-(4-(3,3,3-trifluoropropylsulfonyloxy)phenyl)-1H-imidazole-4-carboxylate (**17**).* A suspension of **16** (5.01 g, 10.13 mmol) in dry CH_2Cl_2 (100 mL) under nitrogen was treated with Et_3N (1.23 g, 12.2 mmol) at rt. The resulting mixture was cooled to −78 °C, and 3,3,3-trifluoropropane-1-sulfonyl chloride (2.19 g, 11.1 mmol) was added dropwise. The reaction mixture was stirred at −78 °C for 3 h, adding more 3,3,3-trifluoropropane-1-sulfonyl chloride (0.28 g 1.43 mmol) after 2 h. Water was added and the phases were separated on a phase separator. The organic phase was concentrated in vacuo to yield the title compound (6.43 g, 97%). ^1H NMR (400 MHz, $CDCl_3$) δ 7.37−7.15 (m, 7H), 5.01 (s, 2H), 3.53−3.45 (m, 2H), 2.84−2.70 (m, 2H), 2.48 (s, 3H). MS m/z 653 (M + H).

*2-(2,4-Dichlorophenyl)-5-methyl-1-(4-(3,3,3-trifluoropropylsulfonyloxy)phenyl)-1H-imidazole-4-carboxylic Acid (**18**).* A solution of **17** (6.43 g, 9.82 mmol) in AcOH (100 mL) was treated with zinc dust (9.74 g, 148.91 mmol). The reaction mixture was stirred at rt for 3 h, after which it was filtered through Celite and evaporated. The residue was dissolved in CH_2Cl_2 and washed with aqueous HCl (0.1 M), dried, filtered, and concentrated in vacuo to yield the crude title compound (5.28 g). MS m/z 523 (M + H).

*4-(2-(2,4-Dichlorophenyl)-4-(4-hydroxycyclohexylcarbamoyl)-5-methyl-1H-imidazol-1-yl)phenyl 3,3,3-trifluoropropane-1-sulfonate (**19**).* A solution of **18** (crude 528 mg) in CH_2Cl_2 (25 mL) was treated with oxalyl chloride (641 mg, 5.00 mmol). A precipitate formed immediately after the addition so more CH_2Cl_2 (15 mL) was added, followed by a few drops of DMF. The reaction mixture was stirred at rt for 2 h,

DOI: 10.1021/acs.jmedchem.7b00861
J. Med. Chem. 2017, 60, 9545−9564

after which more oxalyl chloride (641 mg, 5.00 mmol) was added. After another 10 min the solvents were evaporated. Half of the crude material was suspended in CH_2Cl_2 (5 mL) and added dropwise to a mixture of 4-aminocyclohexanol (74 mg, 0.64 mmol), NaOH (1 M, 10 mL), and CH_2Cl_2 (5 mL). The reaction mixture was stirred at rt for 2 h, after which water/CH_2Cl_2 were added and the phases separated. The organic phase was washed with aqueous HCl (0.1 M) and concentrated in vacuo. The product was purified by HPLC to yield the title compound as a white solid after freeze-drying (164 mg, 54% over 2 steps). Note that the title compound is a mixture of cis- and trans- isomers in a ratio of 0.3:1. ^{1}H NMR (400 MHz, $CDCl_3$) δ 7.33−7.19 (m, 6H), 7.17−7.11 (m, 2H), 7.02 (d, J = 8.4 Hz, 0.6H), 4.07−3.99 (m, 0.3H), 3.99−3.86 (1H, m), 3.66−3.56 (m, 0.6H), 3.52−3.45 (m, 2H), 2.85−2.71 (m, 2H), 2.48 and 2.47 (2s, 3H), 2.12−1.95 (m, 2.6H), 1.81−1.65 (m, 3.8H), 1.49−1.26 (m, 2.7H). HRMS Calcd for $[C_{26}H_{26}Cl_2F_3N_3O_5S + H]$: 620.1001. Found: 620.1002. HPLC: 100%.

*Racemic N-((cis)-2-Aminocyclohexyl)-1-[4-(benzyloxy)phenyl)-2-(2,4-dichlorophenyl)-5-methyl-1H-imidazole-4-carboxamide (**20**).* A suspension of compound **4** (2.00 g, 4.41 mmol) in CH_2Cl_2 (50 mL) was treated with oxalyl chloride (2.80 mg, 22.1 mmol) at rt, followed by one drop of DMF. The mixture was stirred at rt for 30 min, after which the solvents were evaporated under reduced pressure. Half of the amount of the acid chloride (1.04 mg, 2.20 mmol) suspended in CH_2Cl_2 (250 mL) was added dropwise during 31 h to a mixture of (*cis*)-cyclohexane-1,2-diamine (5.00 mg, 43.79 mmol), aqueous NaOH (1 M, 50 mL), and CH_2Cl_2 (50 mL). After the addition was complete, water was added and the phases were separated. The organic phase was washed with aqueous HCl (10%) and brine, dried ($MgSO_4$), filtered, and evaporated to yield the crude title compound (1.31 mg). ^{1}H NMR (400 MHz, $CDCl_3$) δ 8.57 (br s, 2H), 7.69 (br s, 1H), 7.37−6.90 (m, 2H), 5.00 (s, 2H), 4.41 (br s, 1H), 3.72 (br s, 1H), 2.42 (s, 3H), 2.18−1.40 (m, 8H). MS m/z 549 (M + H).

*Racemic N-((cis)-2-Aminocyclohexyl)-2-(2,4-dichlorophenyl)-1-(4-hydroxyphenyl)-5-methyl-1H-imidazole-4-carboxamide (**21**).* A suspension of crude racemic **20** (791 mg, 1.44 mmol) in CH_2Cl_2 (5 mL) and dimethyl sulfide (894 mg, 14.39 mmol) was treated with boron trifluoride (2.04 g, 14.4 mmol). The reaction mixture was stirred at rt for 2.5 days (dark). Water and EtOAc were added and the phases separated. The organic phase was dried ($MgSO_4$), filtered, and evaporated to yield the crude title compound (715 mg). MS m/z 459 (M + H).

*Racemic 4-(4-((cis)-2-Aminocyclohexylcarbamoyl-2-(2,4-dichlorophenyl)-5-methyl-1H-imidazol-1-yl)phenyl 3,3,3-trifluoropropane-1-sulfonate (**22**).* A suspension of crude racemic **21** (715 mg, 1.56 mmol) in CH_2Cl_2 (15 mL) and Et_3N (0.987 g, 9.76 mmol) was treated with TBDMSCl (0.985 g, 6.53 mmol). The reaction mixture was stirred at rt for 22 h. CH_2Cl_2 and water were added and the phases separated. The organic phase was dried ($MgSO_4$), filtered, and evaporated to yield the crude silylated intermediate an oil (1.14 g, 1.99 mmol). MS m/z 573 (M + H). A solution of the crude intermediate (1.14 g, 1.99 mmol) in THF (10 mL) was treated with $(Boc)_2O$ (444 mg, 2.03 mmol). The reaction mixture was stirred at rt for 4 h, after which the solvent was evaporated at reduced pressure and the residue dissolved in CH_2Cl_2. The organic phase was washed with water, dried ($MgSO_4$), filtered, and concentrated in vacuo. The residue was purified by flash chromatography (10−100% EtOAc in heptane) to yield the Boc-protected intermediate (620 mg, yield over 4 steps 70%). ^{1}H NMR (400 MHz, $CDCl_3$) δ 7.37 (d, J = 8.2 Hz, 1H), 7.24−7.08 (m, 3H), 6.85 (d, J = 8.7 Hz, 2H), 6.70 (d, J = 8.7 Hz, 2H), 5.12 (d, J = 4.5 Hz, 1H), 4.32−4.19 (m, 1H), 3.83−3.74 (m, 1H), 2.38 (s, 3H), 1.79−1.39 (m, 8H), 1.33 (s, 9H), 0.87 (s, 9H), 0.11 (s, 6H). MS m/z 673 (M + H). A suspension of the fully protected intermediate (610 mg, 0.91 mmol) in dry THF (3 mL) was treated with TBAF (1.0 M THF, 237 mg, 0.91 mmol). The reaction mixture was stirred at rt for 1 h 45 min. The solvent was evaporated and the residue dissolved in CH_2Cl_2, washed with water, dried ($MgSO_4$), filtered, and evaporated. The residue was dissolved in EtOAc, and some silica gel was added. The suspension was filtered through a plug of silica gel and eluted with EtOAc. The solvent was evaporated to yield the crude desilylated intermediate (529 mg). ^{1}H NMR (400 MHz, $CDCl_3$) δ 7.36 (d, J = 8.1 Hz, 1H), 7.21 (d, J = 1.6 Hz, 1H), 7.13 (d, J = 8.3 Hz, 1H), 7.09 (dd, J = 1.6, 8.3 Hz, 1H), 6.80 (d, J = 8.6 Hz, 2H), 6.68 (d, J = 8.6 Hz, 2H), 5.07 (d, J = 6.6 Hz, 1H), 4.28−4.16 (m, 1H), 3.84−3.72 (m, 1H), 2.32 (s, 3H), 1.55−1.37 (m, 8H), 1.31 (9H, s). MS m/z 559 (M + H). A suspension of the crude intermediate (506 mg, 0.91 mmol) in dry CH_2Cl_2 (6 mL) was treated with Et_3N (110 mg, 1.09 mmol) at rt. The resulting mixture was cooled to −78 °C, and 3,3,3-trifluoropropane-1-sulfonyl chloride (181 mg, 0.92 mmol) in dry CH_2Cl_2 (0.2 mL) was added dropwise. After stirring at −78 °C for 3 h (including extra additions of 3,3,3-trifluoro-propane-1-sulfonyl chloride (2 × 43 mg, 0.22 mmol) after 1.5 and 2.5 h), the reaction mixture was washed with water and evaporated to yield the crude intermediate (655 mg). MS m/z 719 (M + H). To a suspension of the Boc-protected intermediate (655 mg, 0.91 mmol) in MeOH (10 mL) at 0 °C was added dropwise, a solution of thionyl chloride in MeOH (prepared by dropwise addition of thionyl chloride (5.41 g, 45.5 mmol) to MeOH (10 mL) at −40 °C). After the addition, the ice bath was removed. The reaction mixture was stirred at rt for 1 h, after which the solvents were evaporated. The product was purified by HPLC (30−100% CH_3CN (with 0.1% formic acid) in 0.1% formic acid (aq) during 40 min). The CH_3CN was evaporated and the resulting mixture extracted with CH_2Cl_2. The organic phase was washed with aqueous $NaHCO_3$ (1 M), dried ($MgSO_4$), filtered, and concentrated in vacuo to yield the title compound as a slightly yellow solid (315 mg yield over 3 steps 56%). ^{1}H NMR (400 MHz, $CDCl_3$) δ 7.51 (d, J = 8.7 Hz, 1H), 7.32−7.20 (m, 5H), 7.14 (d, J = 8.8 Hz, 2H), 4.20−4.09 (m, 1H), 3.52−3.44 (m, 2H), 3.15−3.06 (m, 1H), 2.84−2.71 (m, 2H), 2.47 (s, 3H), 1.70−1.39 (m, 10H). HRMS Calcd for $[C_{26}H_{27}Cl_2F_3N_4O_4S + H]$: 619.1160. Found: 619.1216. HPLC: 95.4%.

*Racemic 1-(4-(Benzyloxy)phenyl)-2-(2,4-dichlorophenyl)-N-((cis)-2-(dimethylamino)cyclohexyl)-5-methyl-1H-imidazole-4-carboxamide (**23**).* To a suspension of racemic **20** (493 mg, 0.90 mmol) in CH_3CN (10 mL) was added formaldehyde, 36% (135 mg, 4.49 mmol), and sodium borohydride (75 mg, 1.97 mmol) in portions. The suspension was stirred at rt for 2 days, adding 2.5 h afterward sodium borohydride (77 mg, 2.04 mmol), 3.5 h afterward formaldehyde (36% in H_2O, 67 mg, 2.24 mmol), 18.5 h afterward formaldehyde (36% in H_2O, 67 mg, 2.24 mmol), and sodium borohydride (77 mg, 2.04 mmo1) (the temperature was increased to 40 °C for 4.5 h), 23 h afterward AcOH (1.85 mL) at rt, and 28 h afterward formaldehyde (36% in H_2O, 135 mg, 4.49 mmol), followed by sodium cyanoborohydride (112 mg, 1.78 mmol) and 42 h later, formaldehyde (36% in H_2O, (135 mg, 4.49 mmol), followed by sodium cyano borohydride (126 mg, 2.01 mmol). The reaction mixture was diluted with CH_2Cl_2, washed with NaOH (1 M) and brine, dried ($MgSO_4$), filtered, and evaporated. The residue was purified by HPLC (30−100% CH_3CN in aqueous NH_4OAc (0.1 M) over 30 min). The CH_3CN was evaporated and the resulting mixture extracted with CH_2Cl_2, dried ($MgSO_4$), filtered, and evaporated to yield the title compound (163 mg, 32%). MS m/z 577 (M + H).

*Racemic 2-(2,4-Dichlorophenyl)-N-((cis)-2-(dimethylamino)-cyclohexyl)-1-(4-hydroxyphenyl)-5-methyl-1H-imidazole-4-carboxamide (**24**).* A suspension of racemic **23** (163 mg, 0.28 mmol) in CH_2Cl_2 (2 mL) and dimethyl sulfide (351 mg, 5.64 mmol) was treated with boron trifluoride (801 mg, 5.64 mmol). The reaction mixture was stirred at rt for 2 days (dark), adding more of dimethyl sulfide (176 mg, 2.82 mmol) and boron trifluoride (401 mg, 2.82 mmol) after 17 h. Water and CH_2Cl_2 were added and the phases separated. The organic phase was washed with water, dried ($MgSO_4$), filtered, and concentrated in vacuo to yield the crude title compound (104 mg). MS m/z 487 (M + H).

*Racemic 4-(2-(2,4-Dichlorophenyl)-4-((cis)-2-(dimethylamino)-cyclohexylcarbamoyl)-5-methyl-1H-imidazol-1-yl]phenyl 3,3,3-trifluoropropane-1-sulfonate (**25**).* A suspension of racemic **24** (104 mg, 0.21 mmol) in dry CH_2Cl_2 (1.5 mL) was treated with Et_3N (26 mg, 0.26 mmol) at rt. The resulting mixture was cooled to −78 °C, and 3,3,3-trifluoropropane-1-sulfonyl chloride (50 mg, 0.26 mmol) in dry CH_2Cl_2 (0.5 mL) was added dropwise. After stirring at −78 °C for 6.5 h (and adding more 3,3,3-trifluoropropane-1-sulfonyl chloride (2 × 50 mg, 0.26 mmol) after 2 and 4 h, and Et_3N (26 mg, 0.26 mmol) after 4 h), the reaction mixture was washed with water and evaporated. The residue was purified by HPLC (30−100% CH_3CN (with 0.1% formic acid) in 0.1% formic acid over 40 min) and freeze-dried. The product was dissolved in CH_2Cl_2 and washed with $NaHCO_3$ (1 M) and water, dried

DOI: 10.1021/acs.jmedchem.7b00861
J. Med. Chem. 2017, 60, 9545−9564

($MgSO_4$), filtered, and concentrated in vacuo to yield the title compound as a slightly yellow oil (37 mg yield over 2 steps 20%). ^{1}H NMR (400 MHz, $CDCl_3$) δ 7.54 (d, J = 7.6 Hz, 1H), 7.37 (d, J = 8.3 Hz, 1H), 7.31 (d, J = 2.0 Hz, 1H), 7.29 (d, J = 8.9 Hz, 1H), 7.26 (dd, J = 2.0, 8.3 Hz, 1H), 7.17 (d, J = 8.9 Hz, 1H), 4.59−4.51 (m, 1H), 3.56−3.48 (m, 2H), 2.86−2.76 (m, 2H), 2.51 (s, 3H), 2.31 (s, 6H), 2.26−2.19 (m, 1H), 2.07 (dt, J = 3.8, 11.8 Hz, 1H), 2.04−1.96 (m, 2H), 1.85−1.77 (m, 1H), 1.54−1.25 (m, 5H). HRMS Calcd for [$C_{28}H_{31}Cl_2F_3N_4O_4S$ + H]: 647.1473. Found: 647.1472. HPLC: 100%.

*1-(4-(Benzyloxy)phenyl)-2-(2,4-dichlorophenyl)-5-methyl-N-(5-(trifluoromethyl)pyridin-2-yl)-1H-imidazole-4-carboxamide (**26**).* A solution of 2-amino-5-(trifluoromethyl)pyridine (404 mg, 2.49 mmol) in CH_2Cl_2 (2.5 mL) under argon was carefully treated with trimethylaluminum (2.0 M in toluene, 1.25 mL, 2.5 mmol) over 5 min. The solution was stirred at rt for 1.5 h to give a 0.66 M solution of the amidation reagent. A portion of this solution (3.75 mL, 2.5 mmol) was added to compound **3** (400 mg, 0.83 mmol). After stirring at 45 °C overnight, the mixture was cooled to 0 °C and quenched with HCl (aq, 2 M, 7.5 mL). The mixture was diluted with dichloromethane and neutralized by addition of KOH (aq, 2 M). The organic phase was separated, and the aqueous phase was extracted further with dichloromethane. The collected organic phases were washed with H_2O, dried (Na_2SO_4), filtered, and concentrated in vacuo to give a residue which was purified by preparative HPLC to give the title compound (319 mg, 64%) as a solid. ^{1}H NMR (400 MHz, $CDCl_3$) δ 9.91 (s, 1H), 8.57 (s, 1H), 8.52 (d, J = 8.8 Hz, 1H), 7.92 (dd, J = 2.1, 8.8 Hz, 1H), 7.44−7.32 (m, 6H), 7.30−7.21 (m, 2H), 7.04 (d, J = 8.9 Hz, 2H), 6.95 (d, J = 8.9 Hz, 2H), 5.05 (s, 2H), 2.52 (s, 3H). MS m/z 597 (M + H).

*2-(2,4-Dichlorophenyl)-1-(4-hydroxyphenyl)-5-methyl-N-(5-(trifluoromethyl)pyridin-2-yl)-1H-imidazole-4-carboxamide (**27**).* Compound **26** (319 mg, 0.53 mmol) was dissolved in HBr (4.1 M in acetic acid, 7.5 mL, 30.8 mmol) and the mixture stirred at rt for 4 h. The acetic acid was co-evaporated with EtOH and the residue neutralized with ammonia and dissolved in methanol. Purification by flash chromatography gave the title compound (266 mg, 98%). ^{1}H NMR (400 MHz, DMF-d_7) δ 10.36 (s, 1H), 10.09 (s, 1H), 8.89 (d, J = 1.0 Hz, 1H), 8.69 (d, J = 8.9 Hz, 1H), 8.45 (dd, J = 1.0, 8.9 Hz, 1H), 7.85 (d, J = 8.3 Hz, 1H), 7.80 (s, 1H), 7.67 (d, J = 8.3 Hz, 1H), 7.40 (d, J = 8.4 Hz, 2H), 7.06 (d, J = 8.4 Hz, 2H), 2.65 (s, 3H). MS m/z 507 (M + H).

*4-(2-(2,4-Dichlorophenyl)-5-methyl-4-(5-(trifluoromethyl)pyridin-2-ylcarbamoyl)-1H-imidazol-1-yl)phenyl 3,3,3-trifluoropropane-1-sulfonate (**28**).* A mixture of **27** (136 mg, 0.27 mmol) and Et_3N (40 μL, 0.32 mmol) in CH_2Cl_2 (4.0 mL) was cooled to −78 °C then carefully treated with 3,3,3-trifluoropropane-1-sulfonyl chloride (63 mg, 0.32 mmol). The resulting mixture was stirred at −78 °C for 1 h, then allowed to reach room temperature. Water was added to the reaction, and the phases were separated. The organic phase was washed with $NaHCO_3$ and brine, then dried (Na_2SO_4), filtered, and concentrated in vacuo to give a residue which was purified by preparative HPLC to give the title compound (88 mg, 49%) as a solid. ^{1}H NMR (400 MHz, $CDCl_3$) δ 9.87 (s, 1H), 8.55 (s, 1H), 8.49 (d, J = 8.8 Hz, 1H), 7.91 (dd, J = 2.1, 8.8 Hz, 1H), 7.36−7.21 (m, 5H), 7.19 (d, J = 8.8 Hz, 2H), 3.55−3.46 (m, 2H), 2.87−2.71 (m, 2H), 2.54 (s, 3H). ^{13}C NMR (126 MHz, $CDCl_3$) δ 162.0, 154.3, 148.6, 145.6 (q, J = 4.1), 142.7, 137.0, 136.2, 135.6 (q, J = 3.2), 135.2, 134.1, 133.4, 131.0, 130.0, 129.3, 127.9, 127.5, 125.1 (q, J = 277.1), 123.8 (q, J = 271.3), 123.2, 122.1 (q, J = 32.7), 113.1, 44.5 (q, J = 3.3), 29.3 (q, J = 31.5), 11.1. HRMS Calcd for [$C_{26}H_{18}Cl_2F_6N_4O_4S$ + H]: 667.0408. Found: 667.0540. HPLC: 100%.

Biology. *Chemicals and Reagents.* [^{3}H]CP55940 (specific activity 141.2 Ci/mmol) was purchased from PerkinElmer (Waltham, MA). Bicinchoninic acid (BCA) and BCA protein assay reagent were obtained from Pierce Chemical Company (Rochford, IL). Rimonabant was from Cayman Chemical Company (Ann Arbor, MI). CHOK1hCB$_1$_bgal cells (catalogue number 93-0959C2) were obtained from DiscoveRx (Fremont, CA). The membranes (catalogue number RBHCB1M400UA) used for [^{35}S]GTPyS antagonism experiment were purchased from PerkinElmer (Waltham, MA). All other chemicals were of analytical grade and obtained from standard commercial sources.

Cell Culture and Membrane Preparation. CHOK1hCB$_1$_bgal cells were cultured in Ham's F12 Nutrient Mixture supplemented with 10% fetal calf serum, 1 mM glutamine, 50 μg/mL penicillin, 50 μg/mL streptomycin, 300 mg/mL hygromycin, and 800 μg/mL Geneticin in a humidified atmosphere at 37 °C and 5% CO_2. Cells were subcultured twice a week at a ratio of 1:10 on 10 cm diameter plates by trypsinization. For membrane preparation, the cells were subcultured 1:10 and transferred to large 15 cm diameter plates. Membrane fractions were prepared exactly as described before.[50]

Equilibrium Radioligand Displacement Assays. [^{3}H]CP55940 displacement assays on 96-well plate were used for the determination of affinity (IC_{50} and K_i) values of antagonists for the cannabinoid CB_1 receptors. The displacement experiments were performed using six concentrations of competing antagonists in 25 μL of assay buffer (50 mM Tris-HCl, 5 mM $MgCl_2$, 0.1% BSA, pH 7.4) in the presence of another 25 μL of assay buffer with a final concentration of 3.5 nM [^{3}H]CP55940. At this concentration, total radioligand binding did not exceed 10% of that added to prevent ligand depletion. Membrane aliquots containing 5 μg of CHOK1hCB$_1$_bgal membrane in 100 μL of assay buffer were incubated at 30 °C for 60 min. Nonspecific binding (NSB) was determined in the presence of 10 μM rimonabant. Incubation was terminated by rapid filtration performed on 96-well GF/C filter plates (PerkinElmer, Groningen, The Netherlands), presoaked for 30 min with 0.25% PEI (Polyethyleneimine), using a PerkinElmer Filtermate harvester (PerkinElmer, Groningen, The Netherlands). After 30 min of dehydration of the filter plate at 50 °C, the filter-bound radioactivity was determined by scintillation spectrometry using the 2450 MicroBeta^2 plate counter. The binding values were recorded in both counts per minute (CPM) and disintegrations per minute (DPM). Each antagonist was measured in duplicate, and at least three individual experiments were performed.

Classic Radioligand Kinetic Assays. Association experiments were performed by incubating membrane aliquots containing 5 μg of CHOK1hCB$_1$_bgal membrane in a total volume of 100 μL of assay buffer at 30 °C with 3.5 nM [^{3}H]CP55940. The amount of radioligand bound to the receptor was measured at different time intervals during a total incubation of 120 min. Dissociation experiments were performed by preincubating membrane aliquots containing 5 μg of protein in a total volume of 100 μL of assay buffer for 60 min. After the preincubation, radioligand dissociation was initiated by the addition of 10 μM unlabeled rimonabant. The amount of radioligand still bound to the receptor was measured at various time intervals for a total of 240 min to ensure that full dissociation from cannabinoid CB_1 receptor was reached. Incubation was terminated by rapid filtration performed on GF/C filters (Whatman International, Maidstone, UK), presoaked for 30 min with 0.25% PEI, using a Brandel harvester (Brandel, Gaithersburg, MD). Filter-bound radioactivity was determined by scintillation spectrometry using a Tri-Carb 2900 TR liquid scintillation counter (PerkinElmer, Boston, MA).

Competition Association Assays. Kinetic rate index (KRI) values are an average of at least two independent experiments, each consisting of two replicates. Kinetic rate constant values are an average of at least three independent experiments, each consisting of two replicates. The binding kinetics of unlabeled ligands was quantified using the competition association assay based on the theoretical framework by Motulsky and Mahan.[36] A concentration of 1−3-fold of the IC_{50} value was used to determine the binding kinetics of unlabeled CB_1 receptor antagonists. The competition association assay was initiated by adding membrane aliquots (5 μg/well) at different time points for a total of 240 min to a total volume of 100 μL of assay buffer at 30 °C with 3.5 nM [^{3}H]CP55940 in the absence or presence of competing CB_1 receptor antagonists (1 to 3-fold IC_{50}). Incubations were terminated, and samples were obtained as described under Equilibrium Radioligand Displacement Assay. The "dual-point" competition association assays[32] were run similarly, with only two time points, at 30 and 240 min, respectively.

[^{35}S]GTPγS Binding Assays. Antagonism assay: The antagonism of all tested compounds was evaluated at 30 °C in a [^{35}S]GTPγS binding assay as reported earlier.[51] Insurmountability assay: Membrane homogenates containing the CB_1 receptor (5 μg) were equilibrated in the assay buffer (50 mM Tris-HCl, 5 mM $MgCl_2$, 1 mM EDTA, 100 mM NaCl, 0.05% BSA, pH7.4) supplemented with 1 μM GDP, 1 mM DTT, and 5 μg of saponin. Membrane preparations were preincubated with or without antagonists (10-fold K_i values on the CB_1 receptor) for 1 h prior to the

DOI: 10.1021/acs.jmedchem.7b00861
J. Med. Chem. 2017, 60, 9545−9564

challenge of a CB_1 receptor agonist, CP55940 at 25 °C with concentrations ranging from 1 μM to 0.1 nM. Subsequently, [^{35}S]GTPγS (final concentration 0.3 nM) was added and incubation continued for another 30 min at 25 °C. Incubations were terminated, and samples were obtained as described under Equilibrium Radioligand Displacement Assays.

Data Analysis. All experimental data were analyzed using the nonlinear regression curve fitting program GraphPad Prism 6.0 (GraphPad Software, Inc., San Diego, CA). From displacement assays, IC_{50} values were obtained by nonlinear regression analysis of the displacement curves. The obtained IC_{50} values were converted into K_i values using the Cheng–Prusoff equation to determine the affinity of the ligands.[52] The k_{on} and k_{off} values for radiolabeled and unlabeled ligands were fitted and calculated, and the k_{on} and k_{off} values were used to calculate residence times (in min) and kinetic dissociation binding constants (kinetic K_D). Association and dissociation rates for unlabeled compounds were calculated by fitting the data into the competition association model using "kinetics of competitive binding":[36]

$$K_A = k_1[L]\cdot 10^{-9} + k_2$$

$$K_B = k_3[I]\cdot 10^{-9} + k_4$$

$$S = \sqrt{(K_A - K_B)^2 + 4\cdot k_1\cdot k_3\cdot L\cdot I\cdot 10^{-18}}$$

$$K_F = 0.5(K_A + K_B + S)$$

$$K_S = 0.5(K_A + K_B - S)$$

$$Q = \frac{B_{max}\cdot k_1\cdot L\cdot 10^{-9}}{K_F - K_S}$$

$$Y = Q\cdot\left(\frac{k_4\cdot(K_F - K_S)}{K_F\cdot K_S} + \frac{k_4 - K_F}{K_F}\, e^{(-K_F\cdot X)} - \frac{k_4 - K_S}{K_S}\, e^{(-K_S\cdot X)}\right)$$

where k_1 is the k_{on} of the radioligand (M^{-1} s^{-1}), k_2 is the k_{off} of the radioligand (s^{-1}), L is the radioligand concentration (nM), I is the concentration of the unlabeled competitor (nM), and X is the time (min) and Y is the specific binding of the radioligand (DPM). During a competition association, these parameters are set, obtaining k_1 from the control curve without competitor and k_2 from previously performed dissociation assays described under Traditional Radioligand Kinetic Assays. With that, the k_3, k_4 and B_{max} can be calculated, where k_3 represents the k_{on} (M^{-1} s^{-1}) of the unlabeled ligand, k_4 stands for the k_{off} (s^{-1}) of the unlabeled ligand, and B_{max} equals the total binding (DPM). All competition association data were globally fitted. Residence times (RT, expressed in min) were calculated as $RT = 1/(60 \times k_{off})$.

Computational Studies. All computational studies were performed in the Schrödinger suite[53] and based on the crystal structure of the CB_1 receptor co-crystallized with **29** (PDB 5TGZ).[33] The crystal structure was prepared with the Protein Preparation Wizard.[53] Ligands were docked using induced fit docking,[54] with core constraints on the 2,4-dichlorophenyl ring of **29** (all ligands share this moiety). To study whether the difference in RTs among **11d**, **14f**, and **28** could be explained by unfavorable hydration, we generated a WaterMap around **14f**.[47,48] Figures were rendered using PyMol.[55]

■ ASSOCIATED CONTENT

Supporting Information

These materials are available free of charge via the Internet at The Supporting Information is available free of charge on the ACS Publications website at DOI: 10.1021/acs.jmedchem.7b00861.

Target selectivity data for representative human CB_1 receptor antagonists at human CB_2 receptor physicochemical properties of all antagonists, including their correlations with corresponding KRI values; proton NMR spectra for all final products and carbon NMRs spectra of **11b**, **14f**, and **28** (PDF)

Molecular formula strings (CSV)

■ AUTHOR INFORMATION

Corresponding Authors

*For A.P.I.: phone, + 31-71-527-4651; E-mail, ijzerman@lacdr.leidenuniv.nl.

*For R.J.S.: phone, +46-76-140-3140; E-mail, Robert.Sheppard@astrazeneca.com.

ORCID

Adriaan P. IJzerman: 0000-0002-1182-2259

Present Addresses

[‖]For M.J.W.: Northern Institute for Cancer Research, School of Chemistry, Bedson Building, Newcastle University, Newcastle upon Tyne, NE1 7RU, United Kingdom

[⊥]For L.C.: Caltiora Consulting, Gothenburg, Sweden.

[#]For P.S.: Global Product and Portfolio Strategy, Business Development Operations, AstraZeneca, Pepparedsleden 1, Mölndal, 431 83, Sweden

[▽]For R.I.O.: Respiratory, Inflammation and Autoimmunity, IMED Biotech Unit, AstraZeneca, Gothenburg, Sweden

Author Contributions

Lizi Xia and Adriaan P. IJzerman conceived the study. Adriaan P. IJzerman, Robert J. Sheppard, Michael J. Waring, and Laura H. Heitman supervised the project. The chemical synthesis was designed and supervised by Leifeng Cheng and performed by Sara Pahlén, Maria J. Petersson, Peter Schell, and Roine I. Olsson. The bioassays were supervised by Adriaan P. IJzerman and Laura H. Heitman and performed by Lizi Xia and Henk de Vries. The computational work was performed by Eelke B. Lenselink. The manuscript was written by Lizi Xia, Julien Louvel, Robert J. Sheppard, and Adriaan P. IJzerman.

Notes

The authors declare no competing financial interest.

■ ACKNOWLEDGMENTS

The research in this study has been performed in the "Kinetics for Drug Discovery (K4DD)" consortium. The K4DD project is supported by the Innovative Medicines Initiative Joint Undertaking (IMI JU) under grant agreement no. [115366], resources of which are composed of financial contribution from the European Union's Seventh Framework Programme (FP7/2007-2013) and EFPIA companies' in kind contribution. Lizi Xia thanks Dr. Daan van der Es and Ms. Xue Yang for their assistance in preparing the chemistry section and Dr. Frederick W. Goldberg for useful discussions during the preparation of the manuscript. Eelke B. Lenselink would like to thank the Agentschap Innoveren en Ondernemen (AIO) for financial support (AIO project 155028).

■ DEDICATION

[○]We dedicate this study to the memory of Dr. Julien Louvel who passed away on November 5, 2017.

■ ABBREVIATIONS USED

AEA, anandamide; 2-AG, 2-arachidonoylglycerol; CB, cannabinoid; CNS, central nervous system; ECS, endocannabinoid system; GPCRs, G-protein-coupled receptors; KRI, kinetic rate index; PNS, peripheral nervous system; PSA, Polar Surface Area; RT, residence time; SAR, structure–affinity relationship; SKR, structure-kinetic relationship; TMS, tetramethylsilane

■ REFERENCES

(1) Maccarrone, M.; Bab, I.; Bíró, T.; Cabral, G. A.; Dey, S. K.; Di Marzo, V.; Konje, J. C.; Kunos, G.; Mechoulam, R.; Pacher, P.; Sharkey,

DOI: 10.1021/acs.jmedchem.7b00861
J. Med. Chem. 2017, 60, 9545–9564

K. A.; Zimmer, A. Endocannabinoid signaling at the periphery: 50 years after THC. *Trends Pharmacol. Sci.* **2015**, *36*, 277−296.
(2) Pertwee, R. G.; Howlett, A. C.; Abood, M. E.; Alexander, S. P. H.; Di Marzo, V.; Elphick, M. R.; Greasley, P. J.; Hansen, H. S.; Kunos, G.; Mackie, K.; Mechoulam, R.; Ross, R. A. International union of basic and clinical pharmacology. LXXIX. Cannabinoid receptors and their ligands: beyond CB_1 and CB_2. *Pharmacol. Rev.* **2010**, *62*, 588−631.
(3) Munro, S.; Thomas, K. L.; Abu-Shaar, M. Molecular characterization of a peripheral receptor for cannabinoids. *Nature* **1993**, *365*, 61−65.
(4) Abood, M.; Barth, F.; Bonner, T. I.; Cabral, G.; Casellas, P.; Cravatt, B. F.; Devane, W. A.; Elphick, M. R.; Felder, C. C.; Herkenham, M.; Howlett, A. C.; Kunos, G.; Mackie, K.; Mechoulam, R.; Pertwee, R. G. Cannabinoid receptors: CB1 receptor. In *IUPHAR/BPS Guide to Pharmacology*; International Union of Basic and Clinical Pharmacology, May 16, **2017**; http://www.guidetopharmacology.org/GRAC/ObjectDisplayForward?objectId=56 (accessed July 20, 2017).
(5) Pacher, P.; Bátkai, S.; Kunos, G. The endocannabinoid system as an emerging target of pharmacotherapy. *Pharmacol. Rev.* **2006**, *58*, 389−462.
(6) Bermudez-Silva, F. J.; Viveros, M. P.; McPartland, J. M.; Rodriguez de Fonseca, F. The endocannabinoid system, eating behavior and energy homeostasis: the end or a new beginning? *Pharmacol., Biochem. Behav.* **2010**, *95*, 375−382.
(7) Pertwee, R. G. The pharmacology of cannabinoid receptors and their ligands: an overview. *Int. J. Obes.* **2006**, *30*, S13−S18.
(8) Pellicoro, A.; Ramachandran, P.; Iredale, J. P.; Fallowfield, J. A. Liver fibrosis and repair: immune regulation of wound healing in a solid organ. *Nat. Rev. Immunol.* **2014**, *14*, 181−194.
(9) Cinar, R.; Iyer, M. R.; Liu, Z.; Cao, Z.; Jourdan, T.; Erdelyi, K.; Godlewski, G.; Szanda, G.; Liu, J.; Park, J. K.; Mukhopadhyay, B.; Rosenberg, A. Z.; Liow, J.-S.; Lorenz, R. G.; Pacher, P.; Innis, R. B.; Kunos, G. Hybrid inhibitor of peripheral cannabinoid-1 receptors and inducible nitric oxide synthase mitigates liver fibrosis. *J. Clin. Invest. Insight* **2016**, *1*, e87336.
(10) Perkins, J. M.; Davis, S. N. Endocannabinoid system overactivity and the metabolic syndrome: prospects for treatment. *Curr. Diabetes Rep.* **2008**, *8*, 12−19.
(11) *FDA Briefing Document NDA 21-888 Zimulti (rimonabant) Tablets, 20 mg* Sanofi Aventis Advisory Committee, June 13, 2007; http://www.fda.gov/ohrms/dockets/ac/07/briefing/2007-4306b1-fda-backgrounder.pdf (accessed July 20, 2017).
(12) Boekholdt, S. M.; Peters, R. J. G. Rimonabant: obituary for a wonder drug. *Lancet* **2010**, *376*, 489−490.
(13) Topol, E. J.; Bousser, M.-G.; Fox, K. A. A.; Creager, M. A.; Despres, J.-P.; Easton, J. D.; Hamm, C. W.; Montalescot, G.; Steg, P. G.; Pearson, T. A.; Cohen, E.; Gaudin, C.; Job, B.; Murphy, J. H.; Bhatt, D. L. Rimonabant for prevention of cardiovascular events (CRESCENDO): a randomised, multicentre, placebo-controlled trial. *Lancet* **2010**, *376*, 517−523.
(14) Proietto, J.; Rissanen, A.; Harp, J. B.; Erondu, N.; Yu, Q.; Suryawanshi, S.; Jones, M. E.; Johnson-Levonas, A. O.; Heymsfield, S. B.; Kaufman, K. D.; Amatruda, J. M. A clinical trial assessing the safety and efficacy of the CB_1R inverse agonist taranabant in obese and overweight patients: low-dose study. *Int. J. Obes.* **2010**, *34*, 1243−1254.
(15) Aronne, L. J.; Finer, N.; Hollander, P. A.; England, R. D.; Klioze, S. S.; Chew, R. D.; Fountaine, R. J.; Powell, C. M.; Obourn, J. D. Efficacy and safety of CP-945,598, a selective cannabinoid CB_1 receptor antagonist, on weight loss and maintenance. *Obesity* **2011**, *19*, 1404−1414.
(16) de Kloet, A. D.; Woods, S. C. Endocannabinoids and their receptors as targets for obesity therapy. *Endocrinology* **2009**, *150*, 2531−2536.
(17) Sharma, M. K.; Murumkar, P. R.; Barmade, M. A.; Giridhar, R.; Yadav, M. R. A comprehensive patents review on cannabinoid 1 receptor antagonists as antiobesity agents. *Expert Opin. Ther. Pat.* **2015**, *25*, 1093−1116.
(18) Storr, M. A.; Bashashati, M.; Hirota, C.; Vemuri, V. K.; Keenan, C. M.; Duncan, M.; Lutz, B.; Mackie, K.; Makriyannis, A.; Macnaughton, W. K.; Sharkey, K. A. Differential effects of CB_1 neutral antagonists and inverse agonists on gastrointestinal motility in mice. *Neurogastroenterol. Motil.* **2010**, *22*, 787−e223.
(19) Tudge, L.; Williams, C.; Cowen, P. J.; McCabe, C. Neural effects of cannabinoid CB_1 neutral antagonist tetrahydrocannabivarin on food reward and aversion in healthy volunteers. *Int. J. Neuropsychopharmacol.* **2015**, *18*, pyu094.
(20) Copeland, R. A. The drug-target residence time model: a 10-year retrospective. *Nat. Rev. Drug Discovery* **2016**, *15*, 87−95.
(21) Swinney, D. C.; Haubrich, B. A.; Van Liefde, I.; Vauquelin, G. The role of binding kinetics in GPCR drug discovery. *Curr. Top. Med. Chem.* **2015**, *15*, 2504−2522.
(22) Guo, D.; Hillger, J. M.; IJzerman, A. P.; Heitman, L. H. Drug-target residence time—a case for G protein-coupled receptors. *Med. Res. Rev.* **2014**, *34*, 856−892.
(23) Vilums, M.; Zweemer, A. J. M.; Yu, Z.; de Vries, H.; Hillger, J. M.; Wapenaar, H.; Bollen, I. A. E.; Barmare, F.; Gross, R.; Clemens, J.; Krenitsky, P.; Brussee, J.; Stamos, D.; Saunders, J.; Heitman, L. H.; IJzerman, A. P. Structure−kinetic relationships—an overlooked parameter in hit-to-lead optimization: a case of cyclopentylamines as chemokine receptor 2 antagonists. *J. Med. Chem.* **2013**, *56*, 7706−7714.
(24) Guo, D.; Xia, L.; van Veldhoven, J. P. D.; Hazeu, M.; Mocking, T.; Brussee, J.; IJzerman, A. P.; Heitman, L. H. Binding kinetics of ZM241385 derivatives at the human adenosine A_{2A} receptor. *ChemMedChem* **2014**, *9*, 752−761.
(25) Louvel, J.; Guo, D.; Agliardi, M.; Mocking, T. A. M.; Kars, R.; Pham, T. P.; Xia, L.; de Vries, H.; Brussee, J.; Heitman, L. H.; IJzerman, A. P. Agonists for the adenosine A_1 receptor with tunable residence time. A case for nonribose 4-amino-6-aryl-5-cyano-2-thiopyrimidines. *J. Med. Chem.* **2014**, *57*, 3213−3222.
(26) Xia, L.; Burger, W. A. C.; van Veldhoven, J. P. D.; Kuiper, B. J.; van Duijl, T. T.; Lenselink, E. B.; Paasman, E.; Heitman, L. H.; IJzerman, A. P. Structure−affinity relationships and structure−kinetics relationships of pyrido[2,1-f]purine-2,4-dione derivatives as human adenosine A_3 receptor antagonists. *J. Med. Chem.* **2017**, *60*, 7555−7568.
(27) Guo, D.; Heitman, L. H.; IJzerman, A. P. The role of target binding kinetics in drug discovery. *ChemMedChem* **2015**, *10*, 1793−1796.
(28) Cawston, E. E.; Redmond, W. J.; Breen, C. M.; Grimsey, N. L.; Connor, M.; Glass, M. Real-time characterization of cannabinoid receptor 1 (CB_1) allosteric modulators reveals novel mechanism of action. *Br. J. Pharmacol.* **2013**, *170*, 893−907.
(29) Cawston, E. E.; Connor, M.; Di Marzo, V.; Silvestri, R.; Glass, M. Distinct temporal fingerprint for cyclic adenosine monophosphate (cAMP) signaling of indole-2-carboxamides as allosteric modulators of the cannabinoid receptors. *J. Med. Chem.* **2015**, *58*, 5979−5988.
(30) Cheng, L. Midazole-4-carboxamide derivatives for use as cb modulators. WO 2007031721A1, 2007.
(31) Ahlqvist, M.; Cheng, L.; Lundqvist, R.; Sörensen, H. 1,2-Diarylimidazoles for use as cb1 modulators. WO 2007031720A1, 2007.
(32) Guo, D.; van Dorp, E. J. H.; Mulder-Krieger, T.; van Veldhoven, J. P. D.; Brussee, J.; IJzerman, A. P.; Heitman, L. H. Dual-point competition association assay: a fast and high-throughput kinetic screening method for assessing ligand-receptor binding kinetics. *J. Biomol. Screening* **2013**, *18*, 309−320.
(33) Hua, T.; Vemuri, K.; Pu, M.; Qu, L.; Han, G. W.; Wu, Y.; Zhao, S.; Shui, W.; Li, S.; Korde, A.; Laprairie, R. B.; Stahl, E. L.; Ho, J.-H.; Zvonok, N.; Zhou, H.; Kufareva, I.; Wu, B.; Zhao, Q.; Hanson, M. A.; Bohn, L. M.; Makriyannis, A.; Stevens, R. C.; Liu, Z.-J. Crystal structure of the human cannabinoid receptor CB_1. *Cell* **2016**, *167*, 750.e14−762.e14.
(34) Shao, Z.; Yin, J.; Chapman, K.; Grzemska, M.; Clark, L.; Wang, J.; Rosenbaum, D. M. High-resolution crystal structure of the human CB_1 cannabinoid receptor. *Nature* **2016**, *540*, 602−606.
(35) Gustafsson, T.; Ponten, F.; Seeberger, P. H. Trimethylaluminium mediated amide bond formation in a continuous flow microreactor as key to the synthesis of rimonabant and efaproxiral. *Chem. Commun.* **2008**, 1100−1102.

DOI: 10.1021/acs.jmedchem.7b00861
J. Med. Chem. 2017, 60, 9545−9564

(36) Motulsky, H. J.; Mahan, L. C. The kinetics of competitive radioligand binding predicted by the law of mass action. *Mol. Pharmacol.* **1984**, *25*, 1−9.
(37) Packeu, A.; Wennerberg, M.; Balendran, A.; Vauquelin, G. Estimation of the dissociation rate of unlabelled ligand−receptor complexes by a 'two-step' competition binding approach. *Br. J. Pharmacol.* **2010**, *161*, 1311−1328.
(38) Wennerberg, M.; Cheng, L.; Hjorth, S.; Clapham, J. C.; Balendran, A.; Vauquelin, G. Binding properties of antagonists to cannabinoid receptors in intact cells. *Fundam. Clin. Pharmacol.* **2011**, *25*, 200−210.
(39) Labute, P. A widely applicable set of descriptors. *J. Mol. Graphics Modell.* **2000**, *18*, 464−477.
(40) *The ACD Software 12*; Advanced Chemistry Development, Inc.: Toronto, Ontario, Canada, 2015; www.acdlabs.com.
(41) Davis, A. M.; Wood, D. J. Quantitative structure−activity relationship models that stand the test of time. *Mol. Pharmaceutics* **2013**, *10*, 1183−1190.
(42) Hitchcock, S. A.; Pennington, L. D. Structure−brain exposure relationships. *J. Med. Chem.* **2006**, *49*, 7559−7583.
(43) De Vry, J.; Rüdiger Jentzsch, K. Discriminative stimulus effects of BAY 38−7271, a novel cannabinoid receptor agonist. *Eur. J. Pharmacol.* **2002**, *457*, 147−152.
(44) Mauler, F.; Mittendorf, J.; Horváth, E.; de Vry, J. Characterization of the diarylether sulfonylester (−)-(R)-3-(2-Hydroxymethylindanyl-4-oxy)phenyl-4,4,4-trifluoro-1-sulfonate (BAY 38−7271) as a potent cannabinoid receptor agonist with neuroprotective properties. *J. Pharmacol. Exp. Ther.* **2002**, *302*, 359−368.
(45) Horswill, J. G.; Bali, U.; Shaaban, S.; Keily, J. F.; Jeevaratnam, P.; Babbs, A. J.; Reynet, C.; Wong Kai In, P. PSNCBAM-1, a novel allosteric antagonist at cannabinoid CB_1 receptors with hypophagic effects in rats. *Br. J. Pharmacol.* **2007**, *152*, 805−814.
(46) Segala, E.; Guo, D.; Cheng, R. K. Y.; Bortolato, A.; Deflorian, F.; Doré, A. S.; Errey, J. C.; Heitman, L. H.; IJzerman, A. P.; Marshall, F. H.; Cooke, R. M. Controlling the dissociation of ligands from the adenosine A_{2A} receptor through modulation of salt bridge strength. *J. Med. Chem.* **2016**, *59*, 6470−6479.
(47) Abel, R.; Young, T.; Farid, R.; Berne, B. J.; Friesner, R. A. Role of the active-site solvent in the thermodynamics of Factor Xa ligand binding. *J. Am. Chem. Soc.* **2008**, *130*, 2817−2831.
(48) Young, T.; Abel, R.; Kim, B.; Berne, B. J.; Friesner, R. A. Motifs for molecular recognition exploiting hydrophobic enclosure in protein−ligand binding. *Proc. Natl. Acad. Sci. U. S. A.* **2007**, *104*, 808−813.
(49) Mason, J. S.; Bortolato, A.; Weiss, D. R.; Deflorian, F.; Tehan, B.; Marshall, F. H. High end GPCR design: crafted ligand design and druggability analysis using protein structure, lipophilic hotspots and explicit water networks. *In Silico Pharmacol.* **2013**, *1*, 23.
(50) Xia, L.; de Vries, H.; IJzerman, A. P.; Heitman, L. H. Scintillation proximity assay (SPA) as a new approach to determine a ligand's kinetic profile. A case in point for the adenosine A1 receptor. *Purinergic Signalling* **2016**, *12*, 115−126.
(51) Ryberg, E.; Larsson, N.; Sjögren, S.; Hjorth, S.; Hermansson, N. O.; Leonova, J.; Elebring, T.; Nilsson, K.; Drmota, T.; Greasley, P. J. The orphan receptor GPR55 is a novel cannabinoid receptor. *Br. J. Pharmacol.* **2007**, *152*, 1092−1101.
(52) Cheng, Y.-C.; Prusoff, W. H. Relationship between the inhibition constant (K_i) and the concentration of inhibitor which causes 50% inhibition (IC_{50}) of an enzymatic reaction. *Biochem. Pharmacol.* **1973**, *22*, 3099−3108.
(53) *Schrödinger Release 2016-4: MS Jaguar*; Schrödinger, LLC: New York, 2016.
(54) Sherman, W.; Day, T.; Jacobson, M. P.; Friesner, R. A.; Farid, R. Novel procedure for modeling ligand/receptor induced fit effects. *J. Med. Chem.* **2006**, *49*, 534−553.
(55) *The PyMOL Molecular Graphics System, 1.8.3.2*; Schrödinger, LLC: New York, 2016.

DOI: 10.1021/acs.jmedchem.7b00861
J. Med. Chem. 2017, 60, 9545−9564